PHYSICAL REVIEW B **84**, 014522 (2011)

High-field studies of superconducting fluctuations in high-T_c cuprates: Evidence for a small gap distinct from the large pseudogap

F. Rullier-Albenque,[1,*] H. Alloul,[2] and G. Rikken[3]

[1]*Service de Physique de l'Etat Condensé, Orme des Merisiers, CEA Saclay (CNRS URA 2464), F-91191 Gif sur Yvette cedex, France*

[2]*Laboratoire de Physique des Solides, UMR CNRS 8502, Université Paris Sud, F-91405 Orsay, France*

[3]*Laboratoire National des Champs Magnétiques Intenses, UPR 3228, CNRS-UJF-UPS-INSA, F-31400 Toulouse, France*

(Received 11 February 2011; revised manuscript received 1 July 2011; published 28 July 2011)

We have used large pulsed magnetic fields up to 60 T to suppress the contribution of superconducting fluctuations (SCFs) to the *ab*-plane conductivity above T_c in a series of $YBa_2Cu_3O_{6+x}$ from the deep pseudogapped state to slight overdoping. Accurate determinations of the SCF contribution to the conductivity versus temperature and magnetic field have been achieved. Their joint quantitative analyses with respect to Nernst data allow us to establish that thermal fluctuations following the Ginzburg-Landau scheme are dominant for nearly optimally doped samples. The deduced coherence length $\xi(T)$ is in perfect agreement with a Gaussian (Aslamazov-Larkin) contribution for $1.01T_c \lesssim T \lesssim 1.2T_c$. A phase-fluctuation contribution might be invoked for the most underdoped samples in a T range which increases when controlled disorder is introduced by electron irradiation. For all dopings we evidence that the fluctuations are highly damped when increasing T or H. This behavior does not follow the Ginzburg-Landau approach, which should be independent of the microscopic specificities of the superconducting state. The data permits us to define a field $H_c'(T)$ and a temperature T_c' above which the SCFs are fully suppressed. The analysis of the fluctuation magnetoconductance in the Ginzburg-Landau approach allows us to determine the critical field $H_{c2}(0)$. The actual values of $H_c'(0)$ and $H_{c2}(0)$ are found to be quite similar and both increase with hole doping. These depairing fields, which are directly connected to the magnitude of the superconducting gap, do therefore follow the T_c variation which is at odds with the sharp decrease of the pseudogap T^* with increasing hole doping. This is on line with our previous evidence that T^* is not the onset of pairing. So the large gap seen by spectroscopic experiments in the underdoped regime has to be associated with the pseudogap. We finally propose here a three-dimensional phase diagram including a disorder axis, which makes it possible to explain most peculiar observations done so far on the diverse cuprate families.

DOI: 10.1103/PhysRevB.84.014522 PACS number(s): 74.40.−n, 74.72.−h, 74.25.F−, 74.62.En

I. INTRODUCTION

The occurrence of a pseudogap[1] in the phase diagram of high-T_c cuprates has raised many questions which are still intensely debated. Immediately after its discovery, the important issue was to know whether it might be connected to superconductivity (SC). The fact that the onset temperature T^* of the pseudogap has been found quite robust with disorder contrary to T_c has been a strong indication that the two phenomena are not directly related.[2]

While this mainly resulted from quasistatic nuclear magnetic resonance (NMR) measurements in the 1990s, a large amount of new data using energy and/or wave-vector-resolved spectroscopies have followed during the last 10 years. Scanning tunneling microscopy (STM) experiments revealed first that the gap structure detected below T_c in underdoped samples of $Bi_2Sr_2CaCu_2O_8$ (Bi2212) did not totally disappear above, and transforms into a dip in the density of states.[3] From angle-resolved photoemission spectroscopy (ARPES) experiments, it was found as well that a gap structure is observed in the normal state of underdoped samples.[4] The energy gap detected at low T was found to match the T_c variation in overdoped samples, that is, to increase continuously with decreasing doping but to continue to increase in the pseudogap state, when T_c decreases.[3] So putting all these observations in perspective has justified the idea that the pseudogap could be a precursor pairing state and not an independent crossover or ordering occurring in the normal state.

This preformed pair scenario has been strengthened by the observations in the underdoped cuprates of a large positive Nernst heat transport coefficient well above T_c up to an onset temperature T_ν.[5–7] This was attributed to vortices and/or phase fluctuations of the superconducting order parameter, along a line suggested initially from finite-frequency conductivity data.[8] Indeed, in these compounds with small superfluid density n_s, it has been proposed that T_c is determined by the phase stiffness of the superconducting order parameter and can be much lower than the mean-field critical temperature T_c^{MF} (Ref. 9). These experiments, together with the observed diamagnetism above T_c (Refs. 10 and 11) have entertained the idea that a precursor pairing model could be viable to explain the pseudogap. However, others suggest that it could be due to a magnetic order, such as stripes, nematic order, or orbital currents, which could compete or at least interfere with SC.[12–15]

In a previous report, based on the experimental approach using high magnetic fields to suppress the superconducting fluctuations (SCFs), which is described in great detail here, we could determine precisely altogether the onset temperatures T_c' of the SCFs and of the pseudogap T^**within the same set of transport experiments*.[16] We have shown there that T^* occurs below the onset of SCF at optimal doping, demonstrating unambiguously that the pseudogap cannot be a precursor state for superconducting pairing and has then to be related to a distinct magnetic order.

This pseudogap issue being settled, it remains that these Nernst experiments evidence that SC pairing extends above T_c, which raises important questions about the nature and high T extension of the SCFs. Indeed, as for thin superconducting

films the SCFs are expected to extend well above T_c in two-dimensional (2D) systems as compared to the case of classical 3D BCS superconductors, where they disappear in a vanishingly small T range.[17] This has initiated a large effort to study the extension of SCFs in thin metallic films. In particular, it has been demonstrated that a large Nernst signal remains as well above T_c (Ref. 18), displaying strong similarities on the qualitative aspects with what is observed in the cuprates.[19] Therefore, a detailed quantitative study of the SCFs in these systems with short coherence length ξ is highly desirable as it might help as well to clear some issues concerning the SC state in high-T_c cuprates.

Since the early days of SC, one of the simplest ways to study SCFs has been to determine their effect on the electrical conductivity.[17] The fluctuation excess conductivity has been usually well interpreted in the Ginzburg-Landau (GL) formalism in terms of Gaussian amplitude fluctuations of the order parameter.[20] Among the different contributions which can be at play, the Aslamazov-Larkin (AL) term either in 2D or 3D appear to be the most relevant in high-T_c cuprates.[21–24] However, in the majority of experiments reported to date, analyses of the excess conductivity—denoted as paraconductivity in the AL framework—have been limited to optimally doped compounds. Indeed, in this case it has been postulated that the linear T dependence of the resistivity observed in the normal state can be extrapolated down to low T. The SCF contribution to the conductivity has been then estimated by the deviation from this linear behavior. As we demonstrate in this work such an assumption unavoidably introduces large errors if the normal-state resistivity deviates from T linear. Also it is unable to give a reliable estimate of the highest temperature at which SCFs can be detected as this temperature is *a priori* imposed by the analysis. Such a criticism is also valid for the magnetoconductance studies in which the normal-state contribution is either totally neglected[25–28] or accounted for by an approximative extrapolation from the high-T normal-state behavior.[29,30]

Recently, we have proposed an original method based on the behavior of the magnetoresistance in high magnetic fields to determine the field H_c' and the temperature T_c' above which the normal state is completely restored.[31] We have insisted on the fact that T_c' was indeed a reliable determination of the onset of SCF. In the present paper we have been able to improve the data accuracy and to extend the measurements for different hole dopings. This allowed us to perform a quantitative analysis of the SCF contribution to the conductivity, and of its T and H dependence.

After describing the experimental details in Sec. II, we completely determine the normal-state variations of the transport properties in Sec. III. We obtain then accurate determinations of the SCF contribution to the conductivity versus T and H (Sec. IV) both for slightly overdoped and underdoped compounds. The incidence on the SCFs of extrinsic controlled disorder introduced by low-T electron irradiation is studied as well.

In Sec. V we give evidence that T_c' is slightly larger than the onset T_ν of Nernst effect we have taken before on the same samples[7] and that H_c' is comparable to the onset field of SCFs deduced from Nernst signal or diamagnetic contributions to the magnetization.[11]

We then take advantage of this unique set of accurate data to perform a quantitative analysis of the SCF conductivity (Sec. VI). By confronting these results to Nernst measurements, we do establish then (Sec. VI B) that, up to $1.1T_c$, the Gaussian AL contribution which is inversely proportional to $\epsilon = \ln(T/T_c)$ explains quantitatively both data around optimal doping. This approach fails in the case of the most underdoped sample so that contributions of phase fluctuations might be invoked there in a small range of temperatures above T_c (Sec. VI C). Above this range, which increases markedly in presence of disorder, Gaussian amplitude fluctuations of the order parameter again dominate. In any case, for all the samples studied, we obtain an accurate determination of the T dependence of the coherence length $\xi(T)$ and of its $T = 0$ limit.

In Sec. VII, we show that the analysis of the excess magnetoconductivity in the GL regime allows us to estimate the upper-critical fields $H_{c2}(0)$ which are found to increase with doping, similarly to the $H_c'(0)$ values. From this observation, we can conclude that the superconducting gap increases with doping contrary to the pseudogap which decreases.

In Sec. VIII, we study how the SCFs vanish with increasing temperature and magnetic field. We find for all our samples that the SCF magnitude drops sharply at high T to vanish near T_c'. We point out that the cutoff which must be invoked to explain that behavior implies that the density of fluctuating pairs vanishes at T_c'. Moreover, (Sec. VIII B) the field dependence of the SCF conductivity displays a similar and quite robust exponential dependence in H^2, whatever the hole doping or the quantity of disorder. This behavior again suggests that T_c' and $H_c'(T)$ are upper limits fixed by the vanishing of the pair formation energy.

We then discuss in Sec. IX the results obtained in the present paper in the context of the large set of data accumulated on the cuprates in the last decade. We draw there conclusions on various important aspects of the normal-state and SC properties and on the incidence of disorder. We confirm the independence of the pseudogap from the pair formation and give some clues which might help to clarify the one-gap–two-gaps dichotomy in these materials.

II. SAMPLES AND MEASUREMENTS

$YBa_2Cu_3O_{6+x}$ (YBCO) single crystals were grown using the flux method. Low-resistance contacts were achieved by evaporating gold pads in a standard four-probe geometry. Subsequent annealings in different atmospheres were performed in order to get samples with various oxygen contents. We have studied four different samples labeled following the values of their critical temperatures T_c taken at the midpoint of the resistive transition: two underdoped samples UD57 and UD85, an optimally doped sample OPT93.6, and a slightly overdoped one OD92.5. The estimate of the hole doping p has been done using the parabolic relationship between T_c and p (Ref. 32). This yields oxygen contents of 6.54, 6.8, 6.91, and 6.95, respectively. Although this is not a totally secure method,[33] it helps at least to proceed comparisons between data on similar samples. The resistivity curves of the four different samples are displayed in Fig. 1.

The magnetoresistance (MR) measurements were performed at the LNCMI-Toulouse in a pulsed field magnet up

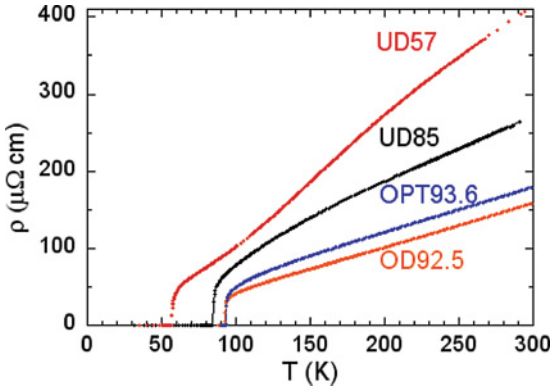

FIG. 1. (Color online) Temperature dependences of the resistivities of the four different pure $YBCO_{6+x}$ samples studied.

to 55–60 T. The magnetic field was applied along the c axis in order to better suppress SC and its polarity was reversed to eliminate by summation any Hall effect contribution to the MR determination.

Controlled disorder was introduced by electron irradiation at low T in optimally doped or underdoped samples with $T_c \sim 57$ K. This type of irradiation provides an efficient way to create point defects, copper and oxygen vacancies, in the CuO_2 planes, uniformly distributed throughout the samples.[34] Their effect on the transport and superconducting properties have been extensively studied previously.[35–37] Whatever the hole doping, we have shown that Matthiessen's rule is well verified at high temperature, as the high-T parts of the $\rho(T)$ curves shift parallel to each other. This confirms that the hole doping is not significantly modified. This type of irradiation results in modifications of the superconducting properties very similar to those obtained with Zn substitution.[33] In particular, the rate of T_c decrease which is around—10 K per defect %—in the CuO_2 plane (Zn impurities or Cu vacancies) in optimally doped $YBCO_7$ becomes twice larger in underdoped $YBCO_{6.6}$ (Refs. 2 and 35).

III. HIGH-FIELD MAGNETORESISTANCE: NORMAL-STATE AND SC CONTRIBUTIONS

Figure 2 shows the tranverse MR curves measured on the OPT93.6 sample for T ranging from above T_c to 150 K. Similar curves are obtained for all the samples studied. At high T, the transverse MR increases as H^2, as better seen in Fig. 3. Such a magnetic-field dependence has been previously observed in different cuprates for $H \leqslant 14$ T (Refs. 38–40). More precisely, in YBCO, Harris *et al.*[39] have shown that the weak field MR $\delta\rho_n/\rho_{n0} = [\rho_n(H) - \rho_n(0)]/\rho_n(0)$ can be expressed as

$$\delta\rho_n(H)/\rho_n(0) = a_{\text{trans}} H^2 \simeq (\omega_c \tau_H)^2 \qquad (1)$$

where $\omega_c = eH/m^*$ is the cyclotron frequency and τ_H is a transverse relaxation time inferred from the Hall angle as $\tan(\Theta_H) = \omega_c \tau_H$. Let us notice here that Eq. (1) refers to the orbital MR coefficient $a_{\text{orb}} = a_{\text{trans}} - a_{\text{long}}$, which would require the knowledge of a_{long}, the longitudinal MR. As this

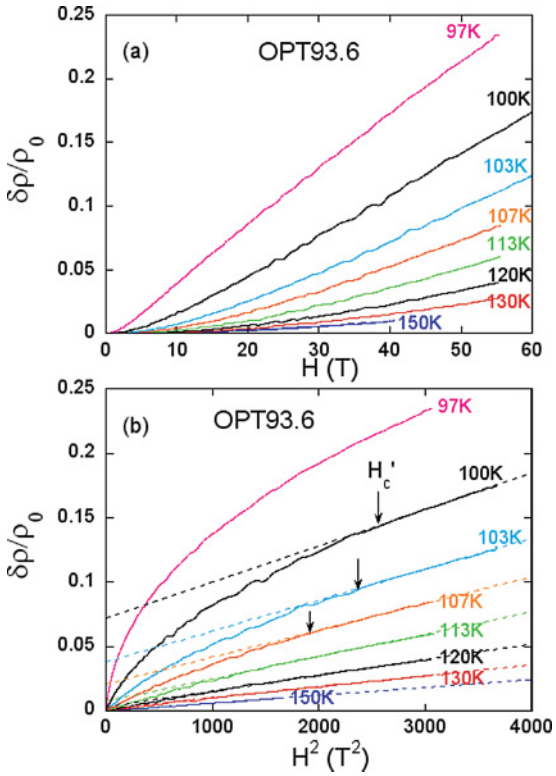

FIG. 2. (Color online) Resistivity increase normalized to its zero-field value plotted versus (a) H and (b) H^2 for temperatures above T_c in the optimally doped sample OPT93.6. For $T \geqslant 140$ K, a H^2 dependence of the MR, represented as dashed lines in (b), is observed for all values of field. For lower T, it is only seen above a given magnetic field H_c' (arrows), which is taken as the threshold field necessary to completely restore the normal state.

latter has been shown to be negligible by Harris *et al.*,[39] we have assumed here that $a_{\text{orb}} \simeq a_{\text{trans}}$. As Hall constant measurements show that $\cot(\Theta_H)$ has a quadratic temperature dependence, this explains the T^{-4} behavior of a_{trans} observed in Ref. 39. The data obtained there in weak magnetic fields are displayed as open symbols in Fig. 4, for optimally doped and underdoped YBCO. At sufficiently high temperature, we

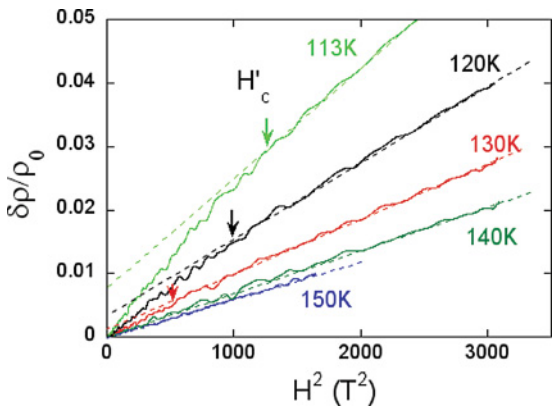

FIG. 3. (Color online) Enlarged view of the variation of the MR in optimally doped sample OPT93.6 which makes it possible to better visualize the deviations from the H^2 normal-state dependence for $T \leqslant 130$ K.

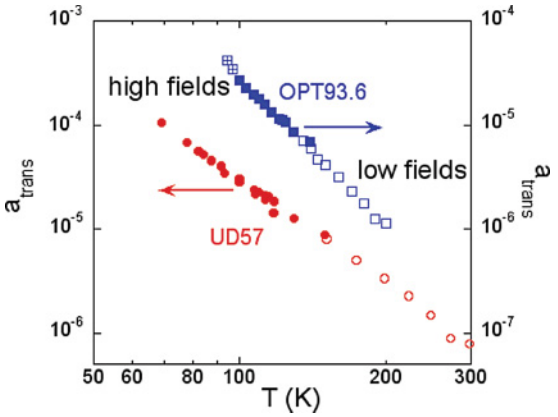

FIG. 4. (Color online) The MR coefficient a_{trans} measured at 55 T (solid symbols) is plotted versus T in logarithmic scales and compared to that obtained at low field and higher T (open symbols), for both optimally doped OPT93.6 and underdoped UD57. Low-field data in this latter case are taken from Ref. 39. In both cases the continuity of the data emphasizes that the magnitude of H has been sufficient to restore the normal state.

also observe a H^2 variation under high magnetic field in our samples. This is illustrated by the H^2 fitting curves in Fig. 2(b) or in Fig. 3 for the OPT93.6 sample. This indicates that the weak field limit still applies in OPT93.6 up to 55 T.

However, large departures with respect to this quadratic behavior appear when T is lowered toward T_c. The MR steadily evolves from a quadratic to a nearly linear field dependence. As stated in Ref. 31, this evolution can be better viewed in the plots versus H^2 of Fig. 2(b) or Fig. 3. There it can be seen that the H^2 variation is still visible for fields exceeding a T-dependent threshold field $H_c'(T)$, which progressively increases with decreasing T. We attribute the initial faster increase of $\delta\rho/\rho$ with H to the destruction of the fluctuating contribution to the conductivity by the applied magnetic field. In such a case the normal-state MR coefficient a_{trans} can then be estimated from the slope of $\delta\rho/\rho$ versus H^2 at our highest available field (55 T). These values of a_{trans} are reported in Fig. 4 together with the values determined at low field (<8 T) on the same sample for $T \geqslant 140$ K. We can see there that the data obtained in high field at low T are in continuity with those obtained at higher T, which emphasizes the validity of our analysis and ensures us that we have effectively completely restored the normal state in high fields for 100 K $\leqslant T \leqslant$ 140 K for the optimally doped sample. However, one can notice in Fig. 4 a small upturn of $a_{trans}(T)$ for $T < 100$ K (crossed squares) which signals that it is no longer possible to totally suppress the superconducting fluctuations even with 55 T at 97 K, that is, 4 K above T_c.

Similar analyses have been done for the OD92.5 and UD85 samples. The $\delta\rho/\rho$ data obtained for the UD57 sample are plotted in Fig. 5 versus H or H^2 in a more limited T range. One can see in Fig. 5(a) the same evolution of the MR as observed for the OPT92.5 sample, from a quadratic to a nearly linear field dependence. However, at ~3 K above T_c, the magnitude of the MR is about a factor three larger in the UD57 sample than in the OPT93.6 one. This comes not only from the larger

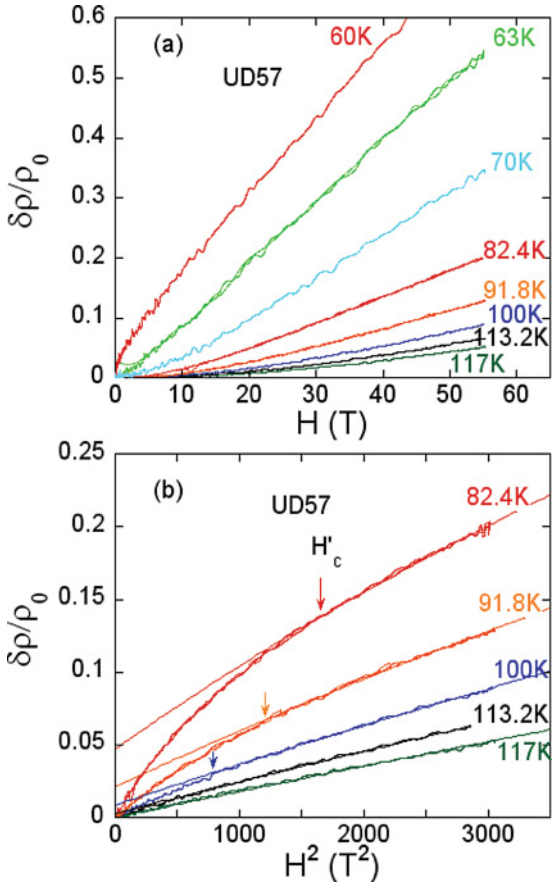

FIG. 5. (Color online) (a) Field variation of the resistivity for decreasing temperatures down to 60 K in UD57. (b) The MR is plotted versus H^2 for 80 K $\leqslant T \leqslant$ 117 K. The full lines are fitting curves using Eq. (2) in the high-field range.

transverse MR in the normal state but also from an enhanced contribution of the SCFs, as we see below.

In such a case one might expect a small saturation of the normal-state MR at large field which can be expressed as[41]

$$\delta\rho_n/\rho_n = \frac{(\omega_c\tau_H)^2}{1+(\omega_c\tau_H)^2}. \quad (2)$$

Equation (2) gives better fits to the normal-state data displayed as full lines in Fig. 5(b) for magnetic fields larger than H_c'. From these fits one can deduce the values for $a_{trans}(T) = (\omega_c\tau_H/H)^2$, which are reported in Fig. 4.[42] They are found here again to be in very good agreement with those obtained in low fields and at higher T by Harris *et al.*[39] The low-T values of $a_{trans}(T)$, slightly larger than in our previous report,[31] are indeed consistent with this small saturation of the MR in the UD57 sample. This analysis improves the accuracy of the determination of $H_c'(T)$ without modifying its magnitude compared to our former data.[31]

Let us finally point out that the behavior of the normal-state MR shown in Fig. 4 is quite similar in the optimal and underdoped case nearly down to T_c and exhibits no sign of the reconstruction of Fermi surface which is observed at lower T for the $YBCO_{6.6}$ (Refs. 43 and 44). This point is discussed in more detail in Sec. IX.

IV. SCF CONTRIBUTION TO THE CONDUCTIVITY

We have shown here above that it is possible to fully recover the normal-state conductivity at temperatures slightly above T_c when the pulsed field exceeds $H_c'(T)$. By extrapolating the normal-state variations of the resistivity $\rho_n(T,H)$ down to zero field, one can thus determine the normal-state value of the resistivity $\rho_n(T,H)$ at each temperature and magnetic field. Consequently, assuming only that a two fluid model applies, it is straightforward to extract the zero-field excess conductivity due to SCFs from

$$\Delta\sigma_{SF}(T,0) = \sigma(T,0) - \sigma_n(T,0) = \rho^{-1}(T,0) - \rho_n^{-1}(T,0). \tag{3}$$

In the main studies of superconducting fluctuations in high-T_c cuprates performed up to date, the determination of the fluctuation excess conductivity has been done in optimally doped samples by assuming that the linear T dependence of the normal-state resistivity observed at high T can be extrapolated down to low temperature. As this assumption can introduce some controversies in the analysis of SCFs—and we show below that it is effectively not correct—the study of the fluctuation magnetoconductivity defined as

$$\Delta\sigma(T,H) = \rho^{-1}(T,H) - \rho^{-1}(T,0) \tag{4}$$

has been often preferred since no assumption on the T dependence of the normal-state transport properties is required in this case.[25] Nevertheless, as the corresponding studies have been performed in rather weak magnetic fields, it has been always admitted that the normal-state MR can be neglected,[25–28] that is, $\sigma_n(T,0) \simeq \sigma_n(T,H)$.

However, for the high magnetic fields used in this study, this assumption is not valid and the normal-state magnetoconductivity has to be taken into account to deduce the field variation of the SCF contribution.[29,30] Within a two-fluid model, we simply write

$$\begin{aligned}\Delta\sigma_{SF}(T,H) &= \sigma(T,H) - \sigma_n(T,H) \\ &= \rho^{-1}(T,H) - \rho_n^{-1}(T,H).\end{aligned} \tag{5}$$

From the relations above the measured total variation of the conductivity is therefore

$$\Delta\sigma_{SF}(T,H) = \Delta\sigma(T,H) + \Delta\sigma_{SF}(T,0) - \Delta\sigma_n(T,H), \tag{6}$$

where the normal-state conductivity is

$$\Delta\sigma_n(T,H) = \rho_n^{-1}(T,H) - \rho_n^{-1}(T,0). \tag{7}$$

This decomposition, which allows us to obtain $\Delta\sigma_{SF}(T,H)$, is illustrated in Fig. 6 for MR data taken at a fixed temperature $T = 85$ K in UD57.

It is worth emphasizing here that the method developed in the present work allows us to determine unambiguously the normal-state contribution in the presence or absence of magnetic field. We have thus been able to analyze separately the variation of $\Delta\sigma_{SF}(T,0)$ with T and that of $\Delta\sigma_{SF}(T,H)$ with H at each T for different hole dopings.

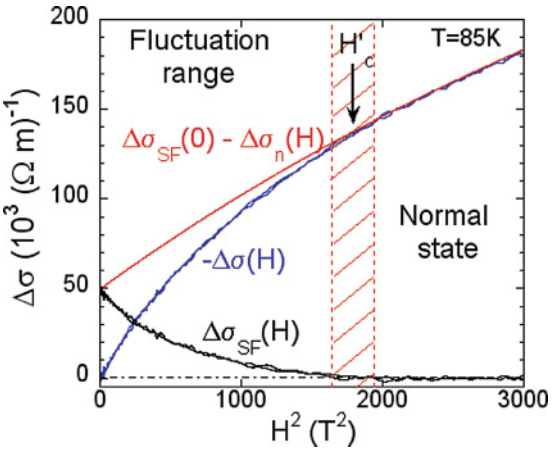

FIG. 6. (Color online) Decomposition of the magnetoconductivity $-\Delta\sigma(H)$ measured at 85 K for the UD57 sample in a normal-state contribution and a superconducting contribution. The zero-field value of $\Delta\sigma_{SF}(H)$ gives the value of the paraconductivity at 85 K.

A. Zero-field excess conductivity versus T: Onset temperature T_c'

Let us first consider the T dependences of the zero-field excess conductivities $\Delta_{SF}(T,0)$ which are reported in Fig. 7 for the four pure samples considered here. One can notice that this quantity dies out very fast with increasing T, which allows us to define an onset temperature T_c'. Given the noise level of the experiments, we have chosen as in Ref. 16 to define T_c' as the temperature where $\Delta\sigma_{SF}(0)$ is lower than $1 \times 10^3(\Omega\,\mathrm{m})^{-1}$, as indicated in the inset of Fig. 7. Let us note that the decrease in $\Delta_{SF}(T,0)$ with temperature is much slower for the most underdoped sample than for the other ones, so that the extension in temperature of the SCFs is larger in this sample than for the other ones.

The variation of T_c' with doping is reported in Fig. 8. The interesting point is that T_c' is only sightly dependent on hole doping and is maximal for optimal doping. We have also reported in this figure the dependence of the

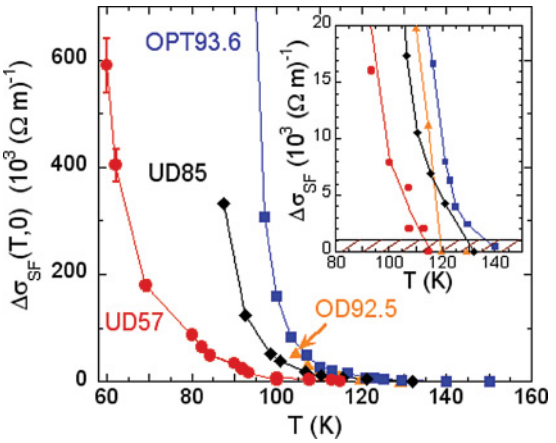

FIG. 7. (Color online) SC fluctuation contribution to the zero-field conductivity $\Delta\sigma_{SF}(T,0)$ for the four YBCO samples studied here (Ref. 45). The enlargement of the high-T range shown in the inset gives an estimate of the accuracy on the determination of T_c', the onset of SC fluctuations. Lines are guides for the eyes.

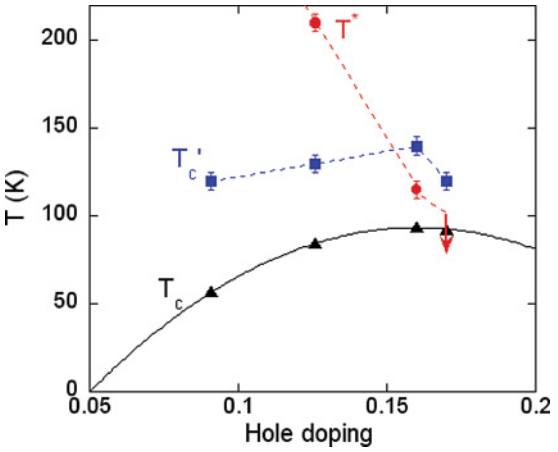

FIG. 8. (Color online) The values of T_c' (squares) and $T^\star$ (circles) are plotted versus the hole doping for the four samples studied. The solid line indicates the superconducting dome. Contrary to T_c' that is rather insensitive to hole doping, $T^\star$ is found to increase with decreasing doping and crosses the T_c' line near optimal doping.[16]

pseudogap temperature $T^\star$ whose determination has been done simultaneously using the same series of experimental data.[16] The fact that the T_c' line crosses the pseudogap line near optimal doping shows unambiguously that the pseudogap phase cannot be a precursor state for the superconducting phase.

The quasi-insensitivity of T_c' to doping observed here appears very different from what is observed by Nernst or magnetization measurements in single-layer materials such as $La_{1-x}Sr_xCuO_4$ (LSCO) or La-doped Bi2201 for which the onset temperature of SCFs is strongly dependent on hole doping with a sharp maximum in the underdoped region.[11] We discuss this point in the discussion Sec. IX in conjunction with the effect of controlled disorder.

B. Field variation of the SF conductivity: Onset field H_c'

In the same way the variation of $\Delta\sigma_{SF}(T,H)$ with magnetic field allows us to analyze how the excess conductivity is destroyed by the applied field. This is exemplified in Fig. 9 for UD85 at 90 K $\leqslant T \leqslant$ 120 K. We can see that $\Delta\sigma_{SF}(T,H)$ starts to decrease quadratically with H whatever T. This H^2 dependence is clearly visible at the highest T for fields up to 30 T. The same behavior is observed for all the samples studied in the small temperature range which can be explored by our method. One can also notice that the accuracy on $\Delta\sigma_{SF}(T,H)$ decreases with increasing field. This is due both to an increase of the noise induced by the stresses on the magnet at the highest field values and a much reduced data-acquisition time in the high-field range. This fixes our noise level at about $1 \times 10^3(\Omega\,\mathrm{m})^{-1}$ at high fields.

We can thus determine the fields $H_c'(T)$ at which $\Delta\sigma$ becomes smaller than this value. As T decreases, it becomes difficult to ascertain that the normal state is fully reached when $H_c'(T)$ becomes comparable to the highest available field. This makes it difficult to deduce precise values of $H_c'(T)$ when they become larger than ∼45 T.

One can see in Fig. 10 that $H_c'(T)$ drops rapidly with increasing T. For all the samples the variation of $H_c'(T)$ appears linear near T_c'. It is then tempting to use a parabolic

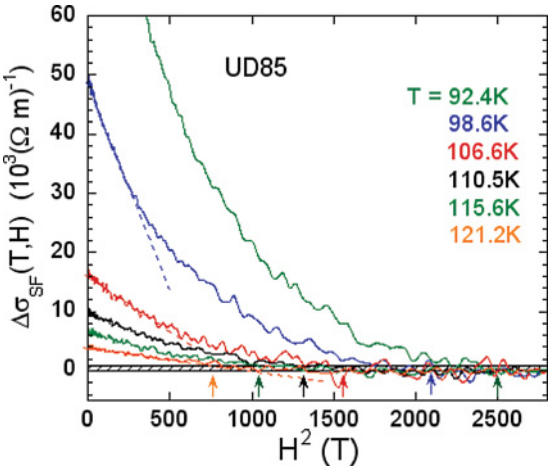

FIG. 9. (Color online) SC fluctuation contribution to the conductivity $\Delta\sigma_{SF}(T,H)$ in UD85 plotted versus H^2. The initial linear decays displayed as dashed lines visualize the quadratic field dependence observed for low magnetic fields. The arrows indicate the threshold fields $H_c'(T)$ taken at $\Delta\sigma_{SF}(T,H) = 1 \times 10^3(\Omega\,\mathrm{m})^{-1}$. The plotted curves correspond to increasing temperatures from top to bottom.

T variation to fit the data as applied for the critical field of classical superconductors:

$$H_c'(T) = H_c'(0)[1 - (T/T_c')^2]. \tag{8}$$

The fitting curves displayed as dashed lines in Fig. 10 give correspondingly an indication of the field $H_c'(0)$ required to completely suppress the SC fluctuation contribution down to 0 K. It is clear that $H_c'(0)$ *increases* with hole doping and reaches a value as high as ∼150 T at optimal doping.

C. Influence of disorder

In cuprates it is now well established that nonmagnetic impurity substitutions or in-plane disorder are detrimental to

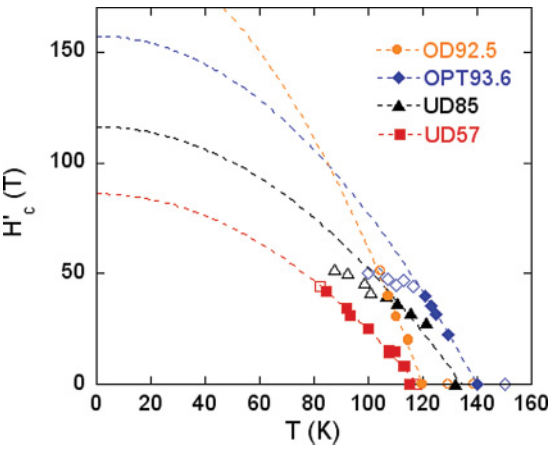

FIG. 10. (Color online) The field H_c' at which SC fluctuations disappear and normal state is fully restored is reported versus T for the four pure samples studied. Dashed lines represent the fitting curves to Eq. (8) using data with solid symbols. When $H_c'(T) \gtrsim 40T$ (open symbols), the data are somewhat underestimated as the maximum applied field is not sufficient.

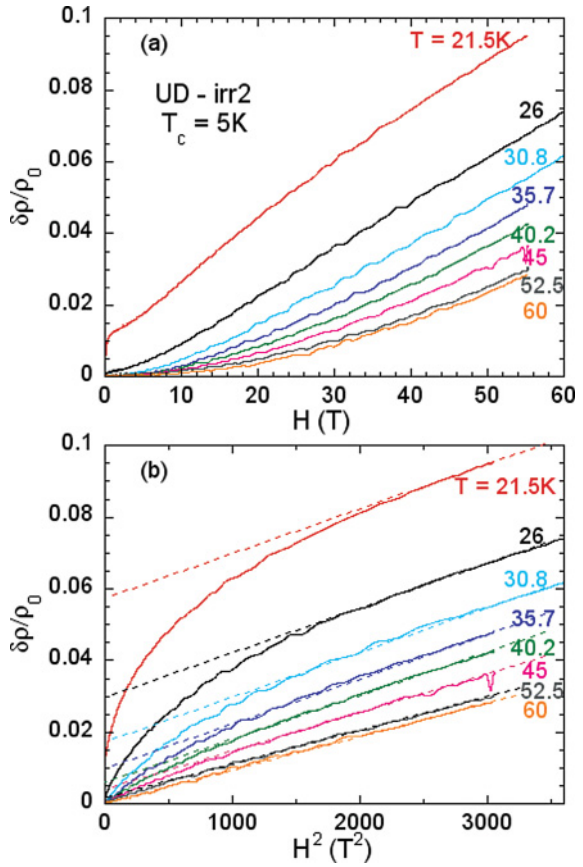

FIG. 11. (Color online) Magnetoresistivity $\delta\rho/\rho_0$ plotted versus H (a) or H^2 (b) for a UD57 irradiated sample with $T_c = 5$ K. Dotted lines give the normal-state behavior restored in high fields. They parallel each other, which points out that the MR and the scattering time τ are nearly T independent for strong disorder.

SC and strongly depress T_c, the temperature of establishment of 3D SC.[33] However, it has been shown as well that the SCFs, as seen by Nernst effect, remain at temperatures much higher than the 3D T_c in disordered samples.[7] So, we expect to detect paraconductivity contributions well above T_c in the presence of disorder. Let us also notice that increasing disorder decreases markedly $\omega_c\tau_H$, which ensures that a H^2 dependence up to 55 T is now perfectly verified for the normal-state MR of irradiated underdoped samples. The magnetoresistivity curves obtained in a UD57 sample in which T_c has been decreased down to 5 K are reported in Fig. 11 versus H or H^2.

It is striking to see that even in this low-T_c sample, a magnetic field larger than 40 T is still necessary to totally suppress the superconducting fluctuations at 21 K, that is, 16 K above T_c. Moreover, we observe that the H^2 term is nearly T independent, which might be quite reasonable in this highly disordered sample for which the relaxation time is expected to become rather T independent. This confirms that the normal-state behavior is totally restored above the threshold field H_c'.

The values of $\Delta\sigma(T,0)$ are reported in Fig. 12(a) for OPT and UD57 samples either pure or irradiated by electron irradiation at low temperature. We notice that the measured SC fluctuation conductivity $\Delta\sigma$ remains of the same order of magnitude as that of the pure samples in both cases. Using the same procedure as described above, we can also determine

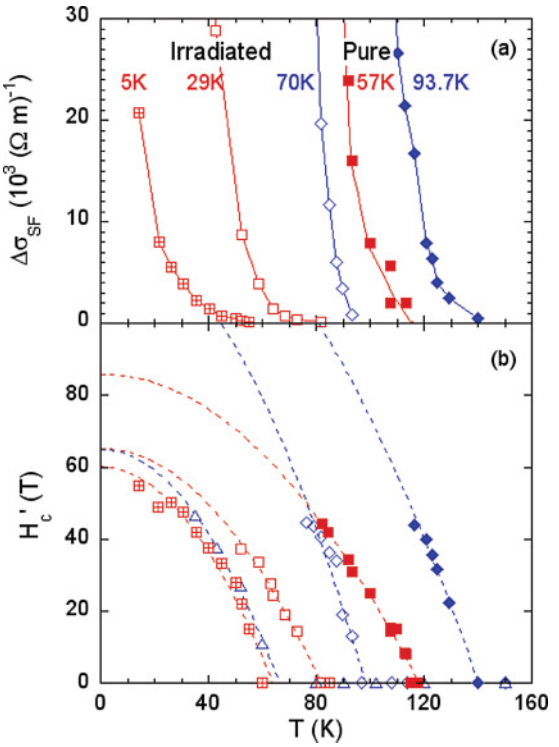

FIG. 12. (Color online) Comparison of the SCF conductivity $\Delta\sigma_{SF}(T,0)$ in (a) and onset field $H_c'(T)$ in (b) for pure (solid symbols) and disordered (open symbols) samples of OPT93.6 (diamonds, triangles) and UD57 (squares), with the reduced T_c values as indicated in (a). In (b) dashed lines are the fitting curves using Eq. (8). Data corresponding to an irradiated OPT sample with $T_c = 30$ K (open triangles) have been added (Ref. 46).

$H_c'(T)$ for the different samples. The corresponding values as well as the fitting curves using Eq. (8) are displayed in Fig. 12(b).

In the case of the most irradiated UD sample with $T_c = 5$ K, we have been able to nearly completely suppress SC with 55 T. The fact that $H_c'(T)$ can be rather well fitted by Eq. (8) somehow validates the use of this equation to fit our other data. In Fig. 13 where the variations of T_c' and $H_c'(0)$ are plotted versus T_c, one can see that both quantities decrease with increasing disorder. The reduction in T_c' nearly follows that in T_c for the underdoped sample while it is slightly larger for the OPT sample. Consequently, when T_c is decreased by disorder, *the relative range of SCFs with respect to the value of T_c expands considerably*. We also observe that $H_c'(0)$ decreases linearly with decreasing T_c, but more rapidly for the OPT samples than for the UD57 ones. In both cases, even for samples with very low T_c, magnetic fields as large as 30–60 T are still necessary to reach $H_c'(0)$, as can be seen in Fig. 13(b).

V. COMPARISON WITH RESULTS OBTAINED BY DIFFERENT EXPERIMENTS

We have shown that high field resistivity measurements above T_c allow us to determine the temperature range as well as the extension in magnetic field of the fluctuation excess conductivity. It is thus very interesting to compare our

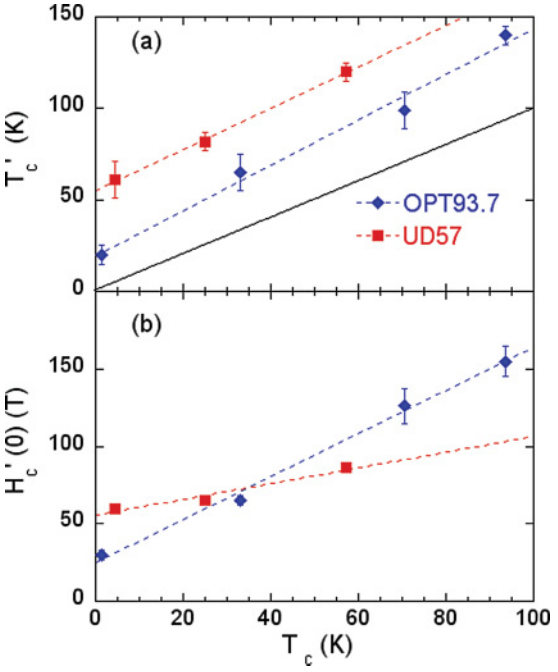

FIG. 13. (Color online) Variations of (a) T_c' and (b) $H_c'(0)$ for OPT (diamonds) and UD (squares) pure and disordered samples versus T_c. Here the T_c value is used to monitor the disorder. The full line in (a) corresponds to a slope unity which parallels the T_c variation. Data from Ref. 46 corresponding to irradiated OPT samples with $T_c = 30$ K and 1.9 K have been added.

results with those obtained by Nernst effect or magnetic torque measurements that have been developed for more than 10 years to probe the presence of SCFs above T_c in high-T_c cuprates.[11]

A. Onset temperature for SCFs

The temperature ranges of SCFs found here are analogous to those measured in pure high-T_c cuprates by these other techniques. For optimally doped YBCO, $T_c' = 135(5)$ K found here is in remarkable agreement with the onset obtained from the diamagnetic response in high fields.[11] The variation with doping is also very similar to that observed in Bi2212 by Nernst effect or diamagnetic measurements.[10] Even though a very small increase of the onset temperature (from 125 K to 130 K) is found upon underdoping in this latter case, contrary to our results, which show a small decrease (from 135 K to 120 K) in the same doping range, *the important point is that T_c' is not found to vary much with doping, contrary to the pseudogap temperature T^*.*

It is worth noting that the values of T_c' found here for the pure compounds are larger than the onsets of Nernst signal measured previously on the same samples.[7] However, one can see in Fig. 14, where the determinations of T_ν and T_c' are compared for the OPT93.6 and UD57 samples, that the criterion used to deduce T_c' is much more precise than that for T_ν. Indeed, a negative T-dependent contribution of the normal-state Nernst signal yields a minimum in α_{xy}/B and hides the real onset of SCFs. It thus appears that the Nernst effect is not the best probe to detect SCFs in the case of YBCO.

In a general way, the measured onset marks the point at which instruments lose sensitivity to detect superconducting

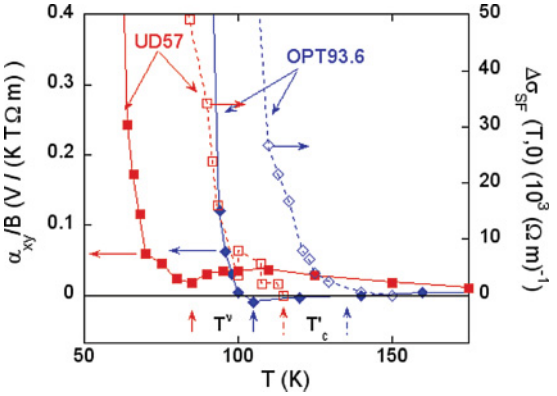

FIG. 14. (Color online) Comparison of the onset temperature for SCFs extracted from Nernst measurements (T_ν) and from this work (T_c') in the same OPT93.6 and UD57 samples. The solid symbols are for the off-diagonal Peltier conductivity deduced from the analysis of the Nernst coefficient (Ref. 7) while the open ones are the values of $\Delta\sigma_{SF}(T,0)$ obtained in this work. The values of T_ν (vertical arrows) had been estimated at temperatures corresponding to the minimal values of α_{xy}/B.

fluctuations. This can explain results of a recent report in which the fluctuation excess conductivity measured by the Josephson effect between an optimally doped YBCO and an underdoped one with $T_c = 61$ K, drops very fast and is found to vanish at $\backsim$15 K above T_c (Ref. 47). In our case, the excess conductivity of the UD57 sample is still 5% of its normal-state contribution at 85 K, that is, 23 K above T_c. Such an explanation might also account for the much smaller fluctuation range determined recently by microwave absorption measurements in YBCO or mercury compounds.[48,49]

We observe that the gap between T_ν and T_c' is progressively reduced when disorder is introduced in the samples. This is due to the fact that the Nernst signal of normal quasiparticles scales inversely with the scattering rate and thus progressively vanishes with disorder, which permits a more accurate determination of T_ν. This results in similar values of T_ν and T_c' in the most irradiated samples.

B. Magnetic field

It is also interesting to compare the H_c' values found here to the maximum magnetic field $H^{\max}$ necessary to completely suppress the Nernst or the diamagnetic signals.[6,10] Although early reports have argued that $H^{\max}$ inferred from Nernst measurements steeply increases with underdoping in Bi2212,[50] more recent studies have shown that this field rather increases with doping, in agreement with what we find here for $H_c'(0)$. In particular, very large values of $H^{\max}$ have been estimated from torque magnetometry in optimally doped Bi2212.[10] At T_c, $H^{\max}$ is equal to 90 T and is thus quite comparable to the value $H_c'(T_c) = 87$ T deduced here for the OPT93.6 sample from the fitting curve displayed in Fig. 10.

One can point out that both values of $H_c'(0)$ and $H^{\max}$ are not determined directly by experiments. Here the $H_c'(T)$ line is only accessible above T_c and the value of $H_c'(0)$ is obtained using Eq. (8). For the Nernst (or magnetization) measurements, the $H^{\max}$ values can be only deduced below T_c by taking the

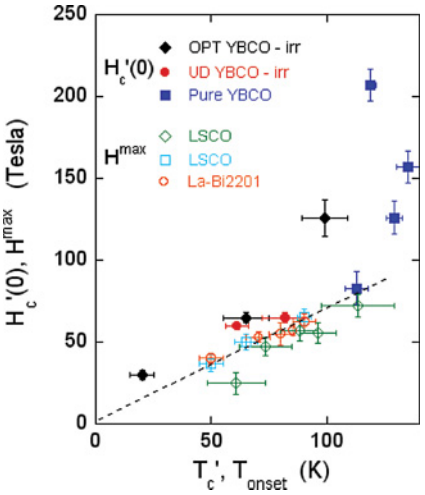

FIG. 15. (Color online) The maximum fields required to completely suppress SC at $T = 0$, as inferred from Nernst, diamagnetism or transport measurements, are plotted versus the onset of superconducting fluctuations for LSCO samples [open diamonds (Ref. 6), open squares (Ref. 51)], La-Bi2201 [open circles (Ref. 51)], and YBCO pure or irradiated crystals (this work). While the results for LSCO, La-Bi2201, and irradiated YBCO samples follow more or less the same linear dependence (dashed line), the $H_c'(0)$ values for the pure UD85, OPT93.6, and OD92.7 are much larger with respect to their T_c'.

extrapolated field at which the Nernst (or diamagnetic) signal should vanish. The fact that similar values of $H^{\max}$ and $H_c'(0)$ are observed in optimally doped Bi2212 and YBCO gives some support to these two determinations.

More generally, a linear variation of these field values versus T_c or T_c' is found when comparing results obtained in low T_c materials like LSCO or La-Bi2201 and our irradiated optimally doped or underdoped YBCO samples as illustrated in Fig. 15. As already proposed,[7,31] this relationship between T_{onset}(or T_c') and $H^{\max}$(or H_c') leads us to speculate that the presence of defects, either intrinsically present or intentionally introduced by irradiation will play here a significant role. It is worth noting that the parameters found for the pure UD57 sample obey the same quasilinear relationship. However, the results obtained for our other pure samples differ markedly from this behavior as larger values of H_c' with respect to their T_c' are found, in agreement with reported $H^{\max}$ value for OP Bi2212.[10] This is of course directly evidenced in Figs. 8 and 10, which show that H_c' increases with hole doping while T_c' remains essentially the same.

The observation of very large values of $H^{\max}$ well above T_c has been taken as the sign that superconducting fluctuations in all high-T_c cuprates originate from vortexlike excitations in a phase-disordered superconductor, rather than fluctuating Cooper pairs.[11] This appears today to be an overstatement. Indeed, recent experiments have evidenced that the Nernst signal in NbSi films can be explained solely in terms of Gaussian fluctuations even in magnetic fields much larger than the orbital upper critical field H_{c2}.[18,52] Moreover, it has been suggested that the Nernst signal of these films could share some resemblances with those seen in cuprates.[19] It is thus very interesting to compare more quantitatively the evolution of the excess fluctuation conductivity with temperature and magnetic field.

VI. QUANTITATIVE ANALYSIS OF THE SUPERCONDUCTING FLUCTUATIONS

As already pointed out, a lot of studies have been dealing with the T dependence of the para conductivity in optimally doped high-T_c cuprates . However, in most experiments the magnitude of $\Delta\sigma_{SF}$ deduced from the data is critically dependent on the behavior taken for the normal-state resistivity, which has been most often taken as linear in T. So, we first emphasize here that our method is particularly adapted to perform a precise quantitative analysis of the excess conductivity since our experimental approach allows us to deduce $\sigma_N(T)$ reliably. We have, for instance, shown in our previous work[16] that the normal-state resistivity of the OPT93.6 sample deviates from the linear T dependence at $T^* \simeq 120$ K due to the opening of the pseudogap. Consequently, the use of a linear extrapolation for the normal-state resistivity would lead to a large overestimate of $\Delta\sigma_{SF}(0)$. To illustrate that, we have therefore mimicked in Fig. 16 the difference generated by such an analysis with respect to our reliable determination using MR data. It is clear that for such a sample the overestimate of $\Delta\sigma_{SF}$ can be quite important. The reliability of the determinations done so far using linear extrapolations of the normal-state conductivity can then be put into question in many cases.

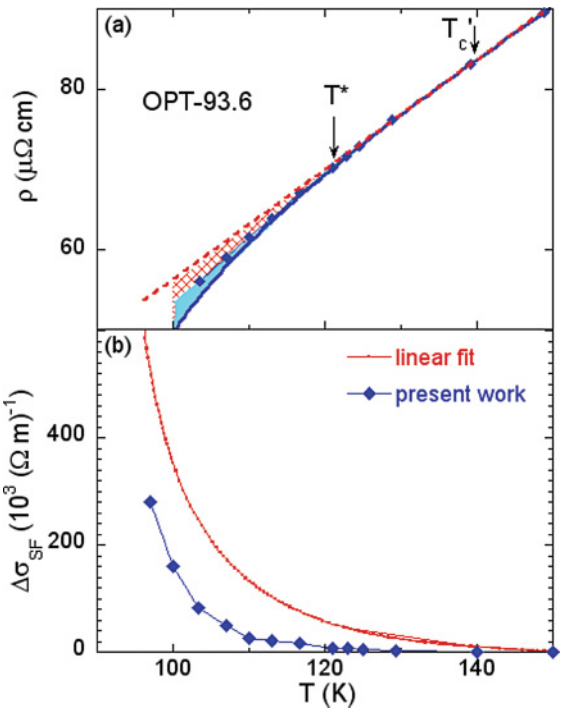

FIG. 16. (Color online) (a) T variations of the zero-field resistivity (solid line) and the normal-state values (symbols) deduced from high-field data for OPT93.6. The colored area corresponds to the range where superconducting fluctuations are effectively present while the hatched area is the extra range found by neglecting the decay of normal-state resistivity due to the pseudogap. (b) The variation $\Delta\sigma_{SF}(T)$ deduced assuming a linear fit would appear more accurate though it overestimates the actual value by at least a factor 3.

A. Contribution of Gaussian fluctuations to paraconductivity

The excess fluctuating conductivity is usually analyzed in the framework of Gaussian fluctuations using the AL theory. As for the Maki-Thompson contribution, which is an indirect contribution arising from the decay of superconducting pairs into quasiparticles and vice versa, it can be neglected in high-T_c cuprates due to strong pair-breaking effects.[53] In the GL theory, the Gaussian fluctuations come from the temporal and spatial fluctuations of the superconducting order parameter. The corresponding paraconductivity is directly related to the temperature dependence of $\xi(T)$, the superconducting correlation length of the short-lived Cooper pairs. Upon cooling down to T_c, ξ is expected to diverge with a power-law dependence given by

$$\xi(T) = \xi(0)/\sqrt{\epsilon}, \tag{9}$$

where $\xi(0)$ is the zero-temperature coherence length and $\epsilon = \ln(T/T_c) \simeq (T - T_c)/T_c$ for $T \gtrsim T_c$. Depending on the relative values of the temperature-dependent perpendicular coherence length $\xi_c(T)$ and of the layer spacing s, the paraconductivity can evolve from a 3D behavior in the immediate vicinity of T_c toward a 2D behavior at larger temperatures.[21] The paraconductivity can be expressed more generally by using the Lawrence-Doniach (LD) theory of layered superconductors as[54]

$$\Delta\sigma^{LD}(T) = \frac{e^2}{16\hbar s}\frac{1}{\epsilon\sqrt{1+2\alpha}}, \tag{10}$$

where the coupling parameter $\alpha = 2[\xi_c(T)/s]^2$, with $\xi_c(T) = \xi_c(0)/\sqrt{\epsilon}$. Sufficiently far from T_c, one expects $\xi_c(T) \ll s$ and Eq. (10) reduces to the well-known 2D AL expression:

$$\Delta\sigma^{AL}(T) = \frac{e^2}{16\hbar s}\epsilon^{-1} = \frac{e^2}{16\hbar s}\frac{\xi^2(T)}{\xi^2(0)}. \tag{11}$$

The only parameters in this expression are the value of the interlayer distance s and the value taken for T_c which can have a huge incidence on the shape of the curve especially for $(T - T_c)/T_c < 0.01$.

We have plotted the variation of $\Delta\sigma_{SF}(T)$ for the four different hole contents as a function of ϵ in Fig. 17. For all the samples except UD57, it is striking to see that our experimental data collapse on a single curve. Moreover, we can see that the data can be fitted reasonably well by the LD expression [Eq. (10)] in the small temperature range $0.03 \leqslant \epsilon \leqslant 0.1$ if one takes $\xi_c(0) \simeq 0.9$ Å. We have assumed here, as usually done, that the CuO_2 bilayer constitutes the basic 2D unit, and s is then taken as the unit-cell size in the c direction: $s = 11.7$ Å. This is a strong indication that *the excess fluctuation conductivity is mainly due to Gaussian fluctuations in these different compounds*. One can see that all the curves in Fig. 17 bend downward very rapidly for $\epsilon \gtrsim 0.1$. This behavior has been pointed out earlier in different fluctuation studies on YBCO.[55–57] It has been proposed that this could be due to the limitations of the GL theory in these compounds with very short coherence lengths. We discuss this point in more detail in Sec. VIII A.

It is clear that the situation is completely different for the UD57 sample for which $\Delta\sigma_{SF}$ is found to be about a factor four larger than for the other dopings. This points to an additional origin of SCFs in this underdoped sample. In fact, we find that the data for this sample can be reconciled with the unique curve found for the other samples by using an effective value T_{c0} different from the actual T_c. This is illustrated in Fig. 17 in which the $\Delta\sigma_{SF}$ data of UD57 are also reported versus $\epsilon = \ln T/T_{c0}$ using $T_{c0} = 72$ K, which is much larger than the actual $T_c = 57.1$ K.

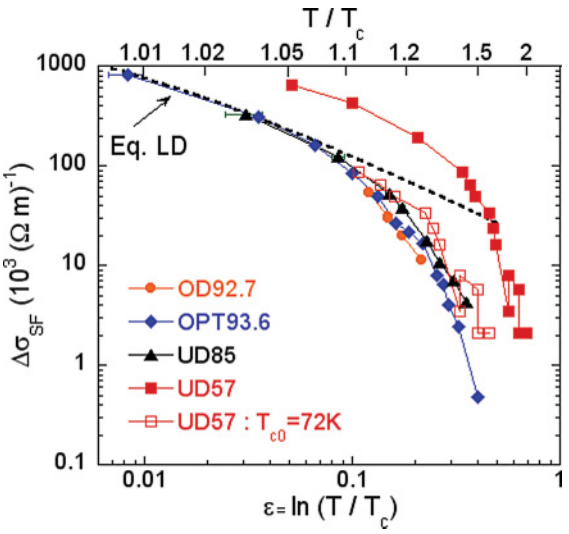

FIG. 17. (Color online) Superconducting fluctuation conductivity $\Delta\sigma_{SF}$ for the four pure samples considered here plotted versus $\epsilon = \ln(T/T_c)$. Values of T_c have been taken here at the midpoint of the resistive transition, and error bars for ϵ using the onset and offset values of T_c are indicated. The dashed line represents the expression of Eq. (10) with $s = 11.7$ Å. and $\xi_c(0) \simeq 0.9$ Å. Full lines are guides for the eye.

The same conclusion has been proposed in Ref. 58 to account for the Nernst signal at high T in underdoped LSCO, which was found to be too large to be explained only by Gaussian fluctuations. In the phase-fluctuations scenario proposed by Emery and Kivelson,[9] this would mean that the actual T_c is suppressed from the mean-field transition temperature T_c^{MF} by phase fluctuations. However, Gaussian fluctuations are still expected above this temperature. Thus, it appears reasonable here to assimilate our effective T_{c0} to T_c^{MF}. Let us notice that this conclusion is in contrast with that argued from paraconductivity measurements in underdoped LSCO samples, in which a description in terms of a 2D AL approach has been proposed to completely account for the experimental data.[59]

It is also interesting to consider the effect of disorder on the paraconductivity. As seen in Fig. 18, the curve found for the disordered optimally doped sample with $T_c = 70$ K nearly falls on that of the pure sample, indicating that here again it is possible to explain the SCFs in the framework of the AL theory. However, this is not the case for the underdoped samples, since their curves are shifted toward larger values of ϵ with increasing disorder. So the introduction of disorder appears to accentuate the difference with the behavior expected from a GL approach. This appears more clearly in the next paragraph.

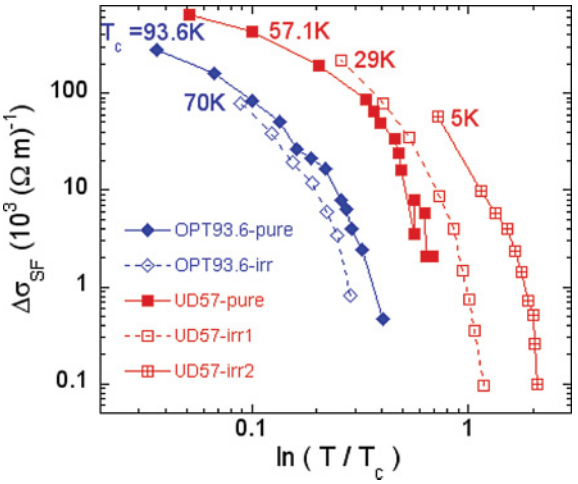

FIG. 18. (Color online) Same as Fig. 17 for the pure and irradiated optimally doped and underdoped $YBCO_{6.6}$ crystals. Solid symbols are for the pure samples while empty ones are for the irradiated ones. The shift to the right observed for the UD57 samples with increasing disorder is shown in Sec. VI C to result from the reduction in T_c with respect to the mean-field temperature T_{c0}.

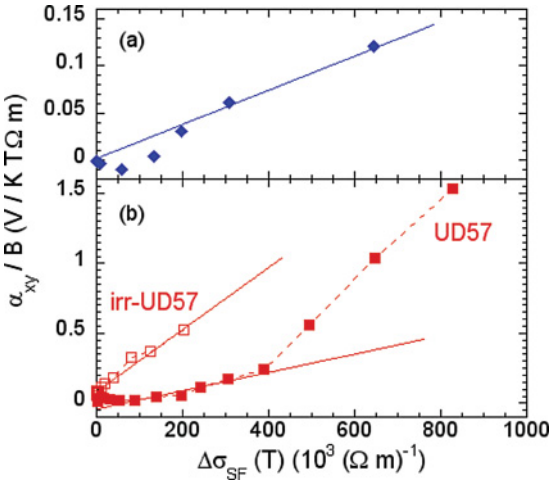

FIG. 19. (Color online) The values of α_{xy}/B taken from Ref. 7 are plotted versus the values of $\Delta\sigma_{SF}(T)$ determined in this work for (a) the pure OPT sample and (b) two UD57 samples pure and irradiated. The values of $\Delta\sigma_{SF}(T)$ reported here have been obtained by interpolation between the data reported in Fig. 17. Solid lines are linear fits for the high T values while the dashed line is guide for the eye for the data near T_c.

B. Nernst effect

In view of the results found above for the paraconductivity, we have found important to analyze as well our Nernst results taken on similar samples[7] along the same lines. The evolution of the off-diagonal Peltier term α_{xy}[60] has already been recalled in Fig. 14 for the pure OPT and UD57 samples. In the 2D GL approach, α_{xy} has been found to follow the simple expression[58]

$$\frac{\alpha_{xy}}{B} = \frac{k_B e^2}{6\pi\hbar^2 s}\xi(T)^2, \tag{12}$$

which shows that α_{xy} is related to the spacing between the layers s and the GL coherence length in the ab plane $\xi(T)$. Consequently, according to Eq. (11), there is a simple linear relationship between α_{xy} and $\Delta\sigma_{SF}(T)$:

$$\frac{\alpha_{xy}}{B} = \frac{8k_B}{3\pi\hbar}\xi(0)^2\Delta\sigma_{SF}(T), \tag{13}$$

whose slope provides a direct determination of the zero temperature coherence length $\xi(0)$. Let us point out that, had we taken the LD term in Eq. (12), it would have been eliminated as the spacing s between layers in this expression (13).

We have tested this relationship first for the optimally doped case and the data are plotted in Fig. 19(a). At high T a negative normal-state contribution to the Nernst signal,[7] apparent in Fig. 14 (similar to that seen by Daou *et al.*[61]), dominates that due to SCFs. Nevertheless, near T_c, this negative counterpart is overcome by the sharp increase of the positive SCF contribution so that the linear relation of Eq. (13) is reliably verified, as can be seen in Fig. 19(a). The linear slope found there near T_c results in a value $\xi(0) \simeq 1.4$ nm after correction for the estimated small negative Nernst contribution.

Using the relationship between $H_{c2}(0)$ and $\xi(0)$,

$$H_{c2}(0) = \Phi_0/2\pi\xi(0)^2, \tag{14}$$

this would lead $H_{c2}(0) \simeq 160$ T, a value which resembles that of $H_c'(0)$ determined above. Consequently, we can conclude that, in optimally doped YBCO, *the paraconductivity and the Nernst signal above T_c are consistent with each other and can be interpreted in terms of Gaussian fluctuations only*, with $\xi(0) \simeq 1.4$ nm.

For the UD57 samples, pure and irradiated with $T_c \simeq 30$ K, the corresponding data are plotted in Fig. 19(b). The same analysis can be done for the pure UD57 sample in the high-T range (above T_{c0}, that is, low values of $\Delta\sigma_{SF}$), where a Gaussian regime is expected to be restored. As can be seen in Fig. 14, the normal-state contribution of the off-Peltier term is positive in this case, so the linear fit of the raw data will give a slightly overestimated value $\xi(0) = 2.0 \pm 0.2$ nm. This would correspond to $H_{c2}(0) \simeq 80 \pm 20$ T, similar here again to $H_c' \simeq 80$ T estimated for this compound.

This conclusion is clearly no longer valid at lower temperatures, near T_c, as the SCF contribution of the off-diagonal Peltier term α_{xy}/B markedly increases with respect to this linear relation. This confirms our previous conclusion that the Nernst data in the pure UD57 sample are not consistent with Gaussian fluctuations for $T_c < T < T_c + 15$ K. We furthermore evidence that, in this range, the positive contributions to the Nernst signal are greatly enhanced with respect to the SCF paraconductivity.

For the irradiated UD57 sample, the quite good linear relationship between α_{xy}/B and $\Delta\sigma_{SF}$ in Fig. 19(b) would correspond to $\xi(0) \simeq 4.3$ nm, hence to a value of $H_{c2}(0)$ as low as 17 T while $H_c'(0) \simeq 60$ T for this compound. This unrealistic value of $H_{c2}(0)$ implies that Eq. (13) does not apply in this case.

This demonstrates that the enhancement of the positive Nernst signal by disorder we evidenced in Ref. 7 is much larger than that of the paraconductivity. This result contradicts the analysis done in Ref. 62 of the Nernst signals in Zn-substituted YBCO thin films.

C. Contribution of phase fluctuations

As an explanation in terms of Gaussian fluctuations is not sufficient to account for the excess conductivity in the UD57 samples, either pure or disordered, it is natural to address the possible role of phase fluctuations. Indeed, in these systems with low carrier density and/or high level of disorder,[9] the low superfluid density is expected to lead to phase fluctuations below the mean-field transition temperature T_c^{MF}. It has been proposed that the superconducting transition is caused by the proliferation of vortices which destroy long-range phase coherence similarly to that predicted for the Kosterlitz-Thouless transition (KT).[63] This would result in a phase-incoherent state with a finite pairing amplitude between T_c and T_c^{MF}. In the framework of the 2D KT transition, the excess conductivity is expressed as

$$\frac{\Delta\sigma}{\sigma_n} \equiv \left(\frac{\xi(T)}{\xi(0)}\right)^2, \tag{15}$$

where the coherence length $\xi(T)$ is now related to the vortex density n_v through $2\pi n_v \equiv 1/\xi^2$. It turns out that a similar relation holds also in the AL regime as shown above [see Eq. (11)], but here $\xi(T)$ is expected to diverge exponentially at T_{KT}. An interpolation formula between these two regimes has been proposed initially by Halperin and Nelson.[64] More recently, Benfatto *et al.*[65] have revisited this problem by means of a renormalization group (RG) approach and have established a direct correspondence between the parameter values used to describe the KT (Kosterlitz-Thouless) fluctuation regime and the reduced temperature τ_c between T_{KT} and T_c^{MF} defined by

$$\tau \equiv \frac{T - T_{KT}}{T_{KT}} \qquad \tau_c \equiv \frac{T_c^{MF} - T_{KT}}{T_{KT}}. \tag{16}$$

They propose an interpolation formula for $T \gtrsim T_{KT}$ which is formally similar to that of Halperin and Nelson:

$$\Delta\sigma_{SF}/\sigma_n = \left(\frac{2}{A}\right)^2 \sinh^2\left(\frac{b}{\sqrt{\tau}}\right), \tag{17}$$

but where the parameters A and b are now obtained from the numerical RG calculations of the correlation length near the transition, so that A is close to unity and b given by $b \sim 2\alpha'\sqrt{\tau_c}$, where α' measures the deviation of the vortex core energy with respect to the conventional value in the XY model.

We have thus tried to fit the data obtained for the SCF conductivity in the pure and irradiated UD57 samples in Fig. 20, where $\Delta\sigma_{SF}/\sigma_n$ are plotted versus T in a semilog scale. Only the very small number of data between $T_{KT} \sim T_c$ and the sharp downturn of $\Delta\sigma_{SF}$ are pertinent in such fits. In the pure UD57 sample, within the foregoing analysis, a natural upper limit for the fit would be $T_{c0} \simeq 72$ K, which could be assimilated to T_c^{MF}. We indeed find that the three significant data make it possible to obtain values for A and b for which the fitted function deviates from the data above T_{c0}. If we take the same criterion to estimate T_c^{MF} in the other samples, we get the values for τ_c reported in Table I. As expected, we find that τ_c increases with disorder, more than a factor 10 between the pure and the most irradiated sample.

It is clear that the limited analysis done above is not sufficient to prove *per se* that the increased magnitude of the SCFs can be attributed to phase fluctuations. Both phase fluctuations and amplitude fluctuations could be emphasized altogether, as claimed by some authors.[66] Hopefully, with the larger pulse fields which become available now, more data points between T_{KT} and T_c^{MF} could become accessible and would make it possible to better test the applicability of Eq. (17) and to get reliable determinations of the different parameters. The fast suppression of the SCFs at high T, similar to that found for the optimally doped samples, is discussed in Sec. VIII A.

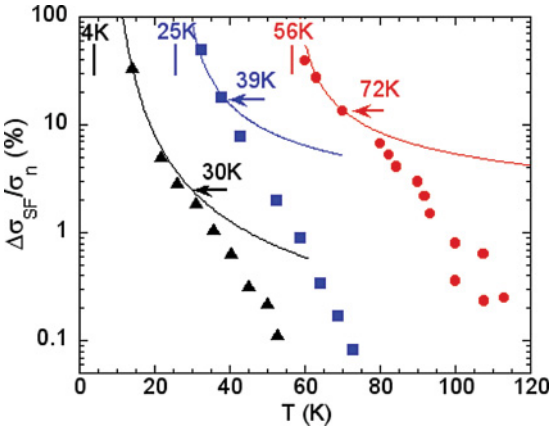

FIG. 20. (Color online) The SCF conductivity normalized to the value in the normal state is plotted versus T for the UD57 samples either pure (circles) or irradiated with T_c values decreased down to 26.8 K (squares) and 11 K (triangles). The vertical bars indicate the estimated values of T_{KT} which are slightly lower than the values of T_c (taken at the midpoint of the superconducting transition). The arrows are for the mean-field temperature T_c^{MF} estimated here from the deviation to the fitting curves using Eq. (17) (solid lines).

VII. FLUCTUATION MAGNETOCONDUCTIVITY

It is also interesting to look more carefully at the way the SCFs are suppressed by the magnetic field. Let us recall here that the dependence of the magnetoconductivity with H and T has been extensively studied in high-T_c cuprates.[25–30] This has been often preferred to the study of paraconductivity as its value is often considered as weakly dependent on the normal-state magnetoconductivity. In fact, this is not really correct even at low magnetic fields since both quantities display inital H^2 variations as shown in Fig. 6. It is thus necessary to subtract the normal-state contribution as expressed in Eq. (6) and to consider the difference

$$\begin{aligned}\Delta\sigma_H(T,H) &= \Delta\sigma(T,H) - \Delta\sigma_n(T,H) \\ &= \Delta\sigma_{SF}(T,H) - \Delta\sigma_{SF}(T,0).\end{aligned} \tag{18}$$

TABLE I. Parameters extracted from the fits of the low-T data of Fig. 20 for the different UD57 samples.

Samples	Pure	irr1	irr2
T_{KT} (K)	56	26.5	4
T_c^{MF} (K)	72	39	30
τ_c	0.22	0.5	2.6
$2\alpha'$	$\simeq$0.5	$\simeq$1	$\simeq$2

Within the GL theory, the evolution of the fluctuating magnetoconductivity with H comes from the pair-breaking effect which leads to a T_c suppression. Different contributions must be taken into account to completely explicit the effect of a magnetic field on the excess conductivity.[26–29,67,68] Nevertheless, it seems legitimate to neglect the Maki-Thompson contribution which already does not contribute to the paraconductivity in zero field. The AL contribution is the sum of two different contributions resulting from interactions of the magnetic field with the carrier orbital (ALO) and spin (Zeeman) degrees of freedom. The former vanishes for applied fields in the ab plane, and the remaining Zeeman term is usually found much smaller than the ALO term for $H//c$ and low-enough magnetic fields.[27,29]

In the layered superconductor model the ALO fluctuation magnetoconductivity can then be written as[27,29]

$$\Delta\sigma_H^{ALO}(T,H) = \frac{e^2}{8\hbar}\frac{1}{h^2}\int_0^{2\pi/s}\epsilon_k\left[\Psi\left(\frac{1}{2}+\frac{\epsilon_k}{2h}\right) - \Psi\left(\frac{\epsilon_k}{2h}\right) - \frac{h}{\epsilon_k}\right]\frac{dk}{2\pi} - \Delta\sigma^{LD}. \quad (19)$$

Here $\epsilon_k = \epsilon[1+\alpha(1-cosks)]$, where α is the coupling parameter defined in Sec. VI A and k is the momentum parallel to the magnetic field H. Ψ is the di-γ function, and $h \equiv H/H_{c2}(0)$. This expression assumes that the temperature dependence of $H_{c2}(T)$ is simply given by

$$H_{c2}(T) = \Phi_0/2\pi\xi(T)^2 = \epsilon H_{c2}(0). \quad (20)$$

This holds as long as the magnetic field variation is set by the size of $\xi(T)$. However, when the magnetic field becomes large enough, the magnetic length $l_B = (\hbar/2eH)^{1/2}$ enters into play and overcomes the variation of $\xi(T)$. The crossover between these two regimes occurs for a field H^* such as

$$H^\star \simeq \epsilon H_{c2}(0). \quad (21)$$

This magnetic field $H^*(T)$ defined above T_c has been called the "ghost critical field" by Kapitulnik *et al.*[69] as it mirrors the upper critical field defined below T_c. For $H > H^*(T)$, the variation with H is governed by the magnetic length l_B as recently evidenced by Nernst measurements in SC disordered films.[52]

In order to analyze the experimental data, we use the procedure described in Ref. 69. We first determine the only adjustable parameter $H_{c2}(0)$ by matching the low-field part of the data for all values of ϵ. We then introduce the higher field values of $-\Delta\sigma_H(T,H)$ computed from Eq. (19), which allows us to define the ghost field $H^\star$ above which a deviation from the experimental data occurs.

This is illustrated for the OPT93.6 sample in Fig. 21 where the evolution of $-\Delta\sigma_H = \Delta\sigma_{SF}(T,0) - \Delta\sigma_{SF}(T,H)$ is plotted versus H at different temperatures ranging from 94.4 K to 103.4 K, corresponding to ϵ values from 0.0085 to ∼0.1. In this temperature range, good fits of the low-field data can be achieved with $H_{c2}(0) = 180(10)$ T. One can also see that the agreement deteriorates at larger fields H^* with increasing temperatures. This is in reasonable agreement with what is expected from Eq. (21), as can be seen in Fig. 22. So, the data follow unambiguously the GL analysis and enable us to determine $H_{c2}(0)$ reliably.

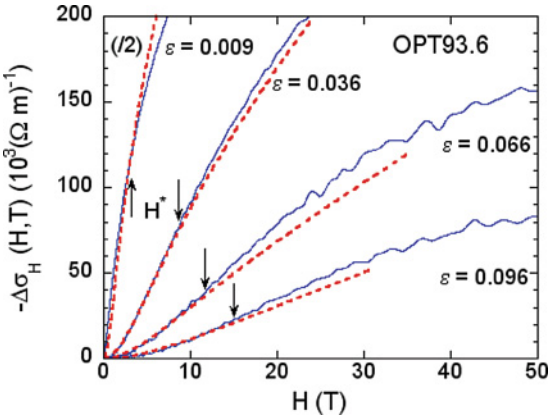

FIG. 21. (Color online) Evolution of the fluctuation magnetoconductivity $-\Delta\sigma_H(T,H) = \Delta\sigma_{SF}(T,0) - \Delta\sigma_{SF}(T,H)$ as a function of H for the OPT93.6 sample at different temperatures, 94.4, 97, 100, and 103.4 K. The dotted lines represent the computed results from Eq. (19) with $H_{c2}(0) = 180(10)$ T. They deviate from the data beyond the $H^\star$ field values shown by arrows and reported in Fig. 22.

At higher T, beyond the GL range deduced from the zero-field SCF conductivity data, the low-field data cannot be matched with Eq. (19) with the same value of $H_{c2}(0)$. One may artificially find a better agreement by increasing $H_{c2}(0)$ with increasing temperature, but this is meaningless and only confirms that Eq. (19) is no longer valid beyond the GL region. So the choice of temperature range used to fit the data can severely affect the deduced value of $H_{c2}(0)$. This might explain why previous attempts to deduce $H_{c2}(0)$ from magnetoconductivity data give contrasting results for optimal doping (those of Ref. 29 are in better agreement with ours than those of Ref. 30).

We could repeat the same procedure for all the dopings studied here, which leads to values of $H_{c2}(0)$ indicated in Table II. In the case of the UD57 sample, the analysis has been performed by assuming that the mean-field temperature is 72 K, as indicated above. As seen in Fig. 23, it is still possible to fit the low-field data reasonably well using Eq. (19) in a T range which is found to slightly exceed the GL regime.

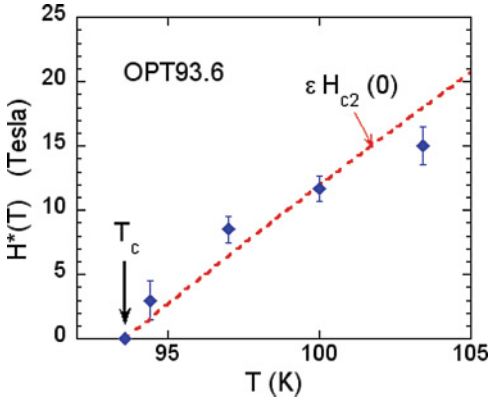

FIG. 22. (Color online) Values of H^* at which Eq. (19) deviates from the experimental results. Those are compared to the expected linear dependence of Eq. (21) using the determined value of $H_{c2}(0) = 180(10)$ T.

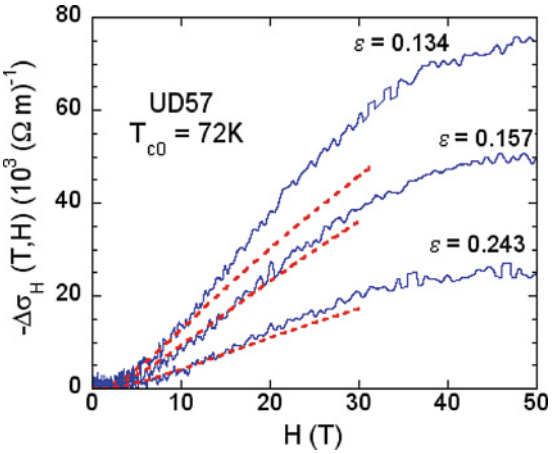

FIG. 23. (Color online) Evolution of the fluctuation magnetoconductivity $-\Delta\sigma_H(T,H) = \Delta\sigma_{SF}(T,0) - \Delta\sigma_{SF}(T,H)$ as a function of H for the UD57 sample at different temperatures, 82.4, 84.2, and 91.8 K. The dotted lines represent the computed results using Eq. (19) with $T_{c0} = 72$ K and $H_{c2}(0) = 90 \pm 10$ T.

We notice that the $H_{c2}(0)$ values determined in this way are surprisingly close to those obtained for $H_c'(0)$ in a totally different way in Sec. IV B, which are reported as well in Table II.

The very important result of this analysis is to unambiguously show that $H_{c2}(0)$ increases and thus $\xi(0)$ decreases with increasing doping in YBCO.

The coherence length is related to the superconducting gap Δ_{SC} through

$$\xi(0) = \beta\left(\frac{\hbar v_F}{\pi\Delta_{SC}}\right), \tag{22}$$

with $\beta = 1$ for s-wave superconductors. By assuming that the Fermi velocity v_F is weakly dependent on doping as found in different cuprates[70] and equal to[71] $v_F \simeq 2.2\ 10^5$ m s^{-1}, we obtain the values of $2\Delta_{SC}/\beta$ indicated in Table II. Independently of the precise value of β, our results demonstrate that the superconducting gap is closely related to T_c in the doping range ~0.09 to ~0.17 considered here.

Recent STM measurements have shown that $\Delta_{SC} \simeq$ 20 meV for an overdoped Bi2212 sample with $T_c = 63$ K,[72] yielding a ratio $2\Delta_{SC}/k_BT_c = 7.4$. A similar ratio is also found for the "small" gap $\Delta = 6.7 \pm 1.6$ meV identified in the STM spectra of an underdoped Bi2201 sample with $T_c = 15$ K.[73] We notice that for $\beta = 1$ in Eq. (22), the data of Table II would also correspond to a similar gap magnitude $2\Delta_{SC} \simeq 8k_BT_c$ whatever the doping. This is a strong indication that the gap determined here can thus be assimilated to the "small" gap detected recently by different techniques.[74]

TABLE II. Values of $H_{c2}(0)$ extracted from the fluctuation magnetoconductivity. They are very close to the values of $H_c'(0)$ determined in Sec. IV B. The values of $\xi(0)$ are calculated from $H_{c2}(0)$ using Eq. (14). The respective values of the superconducting gap Δ_{SC} are estimated from Eq. (22).

Samples	UD57	UD85	OPT93.6	OD92.5
$H_{c2}(0)$ (T)	90(10)	125(5)	180(10)	200(10)
$H_c'(0)$ (T)	86(10)	115(15)	155(10)	207(10)
$\xi(0)$ (nm)	1.9	1.60	1.33	1.26
$2\Delta_{SC}/\beta$ (meV)	46	50	66	69.5

VIII. SUPPRESSION OF SC FLUCTUATIONS BY TEMPERATURE OR MAGNETIC FIELD

We shall consider now more specifically the sharp decrease of SCFs found versus temperature in Fig. 17 and the onset of SCFs at T_c' and H_c'.

A. Temperature

Within the GL description, there is *a priori* no upper temperature limit for the existence of fluctuations, which are expected to survive far above T_c in the normal state. However, it has been pointed out very early that a rapid attenuation of the fluctuations may occur for $T \gg T_c$ in short coherence-length systems, as the GL theory can be put into question when $\xi(T)$ becomes comparable to the zero-temperature in-plane coherence length $\xi(0)$.[55–57] It has been first argued that a short-wavelength cutoff should be taken into account in the fluctuation spectrum. An extension of the AL theory in the 2D case taking this cutoff into account[75] gives a T dependence of the superconducting fluctuation conductivity as

$$\Delta\sigma_{SF}(T) = \frac{e^2}{16\hbar s} f(\epsilon) = \sigma_0 f(\epsilon), \tag{23}$$

where the function $f(\epsilon)$ matches the $1/\epsilon$ first-order expression up to $\epsilon \simeq 0.18$ but deviates then to reach the asymptotic limit[76] $f(\epsilon) \propto 1/\epsilon^3$. Our data can be fitted using the function $f(\epsilon)$ up to $\epsilon \simeq 0.15$. However, as shown in Fig. 24, it then drops much faster well below the expected ϵ^{-3} dependence, above temperatures corresponding to coherence lengths $\xi(T) \lesssim 3\xi(0)$.

Other authors have proposed that a "total-energy" cutoff[77,78] should be more appropriate to describe the evolution

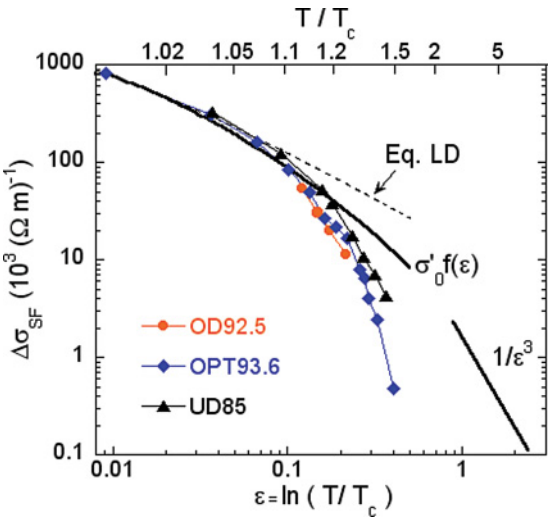

FIG. 24. (Color online) Comparison of the temperature dependence of $\Delta\sigma_{SF}$ for the OD92.5, OPT93.6, and UD85 samples with Eq. (23) (solid line) that takes into account short-wavelength cutoff in the fluctuation spectrum.[75,76] The dashed line is for the LD expression [Eq. (10)].

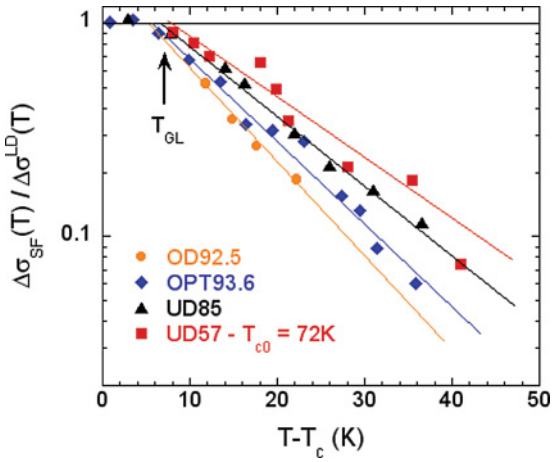

FIG. 25. (Color online) The ratio $\Delta\sigma_{SF}(T)/\Delta\sigma_{LD}(T)$ is plotted versus $T - T_c$ in a semilogarithmic scale for all the pure samples studied. $\Delta\sigma_{LD}(T)$ is calculated from Eq. (10) using the value of $\xi_c = 0.89$ Å determined in Sec. VI A. T_{GL} indicates the upper bound for the GL regime. In the case of the most underdoped UD57 sample, we have assumed that the phase-fluctuation regime disappears at $T_{c0} = 72$K (see Sec. VI). The full lines are exponential fits of the data above T_{GL}.

of the paraconductivity in the high-ϵ region. They assigned its origin to the intrinsic constraint that SCFs cannot survive when the coherence length $\xi(T)$ becomes comparable to the superconducting coherence length ξ_0. They proposed then to mimic this effect using a phenomenological expression which can be transformed into

$$\Delta\sigma_{SF}(T) \simeq \Delta\sigma^{LD}\left(1 - \frac{\epsilon\sqrt{1+2\alpha}}{\epsilon^C}\right)^2, \qquad (24)$$

where $\epsilon^C = \ln(T^C/T_c)$. Our data in YBCO unambiguously allowed us to demonstrate that SCFs are heavily, if not totally, suppressed at high T, which allowed us to define a temperature T_c' above which their detection becomes nearly impossible. This T_c' value could, in principle, be obtained as well using the phenomenological Eq. (24). However, this equation privileges the cutoff behavior and does not reproduce the low-T regime where we have established the validity of the GL approach.

In order to analyze more precisely the attenuation of the superconducting fluctuations with temperature, we have therefore plotted in Fig. 25 the values of $\Delta\sigma_{SF}(T)$ normalized to those expected from the LD formula versus $T - T_c$ in a semilogarithmic scale. For all the samples, we observe that the SCF conductivity vanishes exponentially for $T > T_{GL}$, as

$$\Delta\sigma_{SF}(T) = \Delta\sigma^{LD}(T)\exp\left(-\frac{T - T_{GL}}{T_0}\right). \qquad (25)$$

Here T_{GL}, the upper temperature for the GL regime, exceeds T_c of about 5 K to 7 K. Let us recall here that, for the most underdoped sample, we have replaced T_c with $T_{c0} = 72$ K, the mean-field temperature determined above. The exponential decay rate T_0 of the SCF increases from 10 K to 15 K with decreasing doping.

In our previous report,[31] we had proposed that the total suppression of SCFs in the cuprates could be associated with an intrinsic ultimate possibility to thermally induce pairs in these systems. The simultaneous analysis of the Nernst, paraconductivity, and magnetoconductivity data allows us to emphasize that $\xi(0)$ is intrinsically very small in these compounds and of the same order as the mean distance d between the hole carriers, which is about 10 Å for instance in optimally doped cuprates with a hole content of 0.16 per Cu. Therefore, pairing with shorter coherence length scale would correspond to a thermal excitation of isolated Bose pairs. The total suppression of paraconductivity and Nernst signals above T_c' therefore means that the density of such excited pairs drops to zero already at T_c'. This fits with the idea that the energy of fluctuations which can be thermally excited is bounded with a sharp cutoff at an energy $k_B T_c'$.

In usual BCS materials, for which the density of carriers per atom is of the order of unity, ξ is large enough with respect to the atomic distance a, so that SCFs could be thermally excited as long as $\xi(T) \gg a$, which agrees with the observation that SCFs survive up to at least $T \simeq 30T_c$ in amorphous superconducting films.[18]

The existence of such a sharp cutoff at T_c' is not restricted to pure samples but also applies to disordered ones. This similarity appears very clearly in Fig. 20 for the underdoped irradiated samples where the excess conductivity above T_{c0} nearly parallels that of the pure sample and vanishes exponentially with the same decay rate.

It is quite intriguing to see this quasi- "universality" of the SCF attenuation in a T range where one would rather expect a response highly sensitive to the peculiar features of the systems of interest. This exponential decay means that a T range of the order of $5T_0$ is universally required to suppress the fluctuations above T_c, or T_{c0} in the underdoped cases. Independently of the physical meaning of this representation, this shows that the SCFs vanish similarly with increasing T for all the hole contents. This confirms that the pseudogap state has *no specific incidence on the range of SCFs*. This observation contradicts the recent proposition[79] which attributes the rapid suppression of superconducting fluctuations evidenced by Nernst effect and conductivity measurements in underdoped LaSrCuO[6,59] to the presence of the pseudogap. All the detailed analysis of the data proposed here rather substantiates the conclusion done previously from the simple comparison of the T_c' and $T^\star$ lines[16] that *these two lines are emphasizing two independent phenomena in the phase diagram of cuprates*.

B. Magnetic fields

In the analysis of the fluctuation magnetoconductivity done above, we have been able to fit the data using Eq. (19) as long as $H \lesssim H^*$ for which the GL coherence length $\xi(T)$ becomes comparable to the magnetic length l_B.

Well beyond the GL regime, for $\epsilon \gtrsim 0.2$, where the coherence length is strongly reduced by temperature, we expect that the fluctuation magnetoconductivity cannot be described any longer by Eq. (19). Some data taken in this regime are illustrated in the case of the UD85 sample in Fig. 26(a).

There it can be seen that the excess conductivity appears to decay exponentially with the magnetic field as

$$\Delta\sigma_{SF}(T,H) = \Delta\sigma_{SF}(T,0)\ \exp[-(H/H_0)^2]. \qquad (26)$$

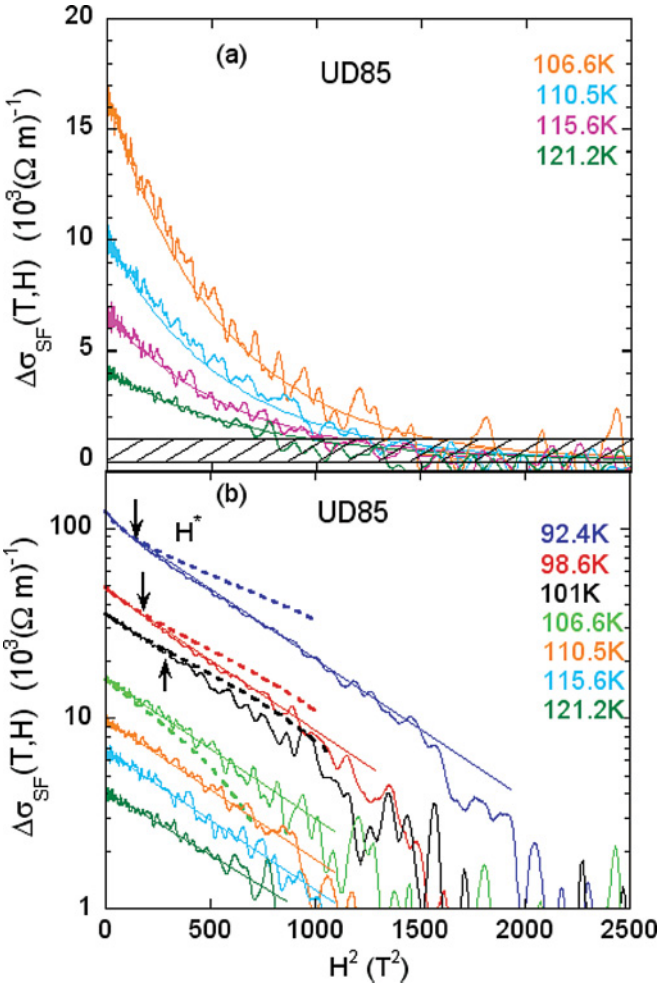

FIG. 26. (Color online) SC fluctuation contribution to the conductivity $\Delta\sigma_{SF}(T,H)$ plotted versus H^2 for the UD85 sample. In (a), the data plotted in a linear scale for the high-T regime can be fitted by the exponential relationship of Eq. (26) with $H_0 \simeq 25$ T. In (b), the data are plotted in a semilogarithmic scale for all the temperatures investigated. The dotted lines are curves using Eq. (19) with $H_{c2}(0) = 125(5)$ T, which deviate from the experimental data for $H > H^\star$ indicated by arrows. The straight lines are exponential fits of the high-field data with $H_0 = 25 \pm 3$ T whatever T. The plotted curves correspond to increasing temperatures from top to bottom.

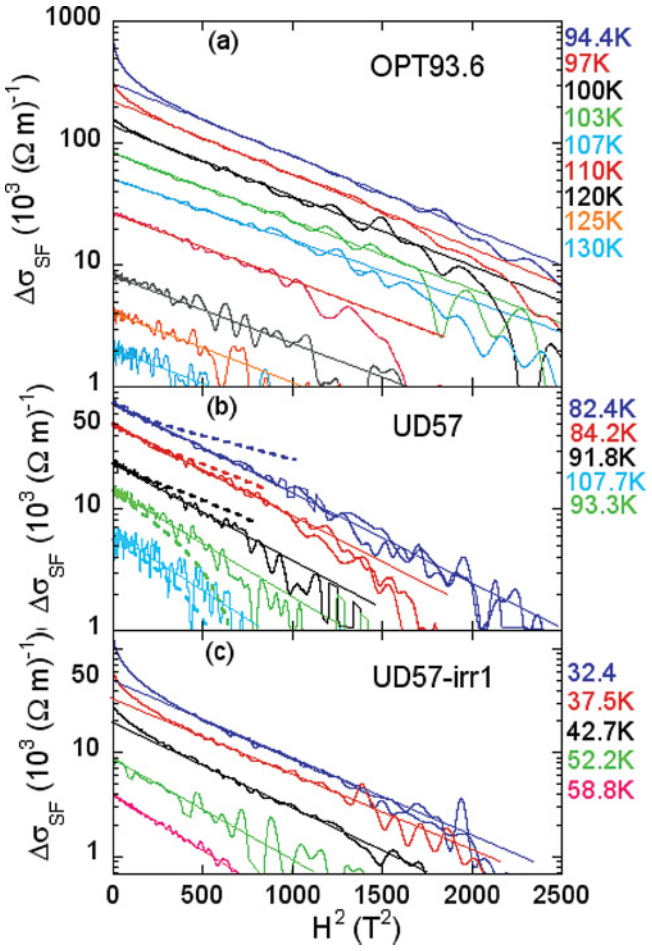

FIG. 27. (Color online) SC fluctuation contribution to the conductivity $\Delta\sigma_{SF}(T,H)$ plotted versus H^2 in a semilog scale for (a) the OPT93.6 sample, (b) the UD57 sample, and (c) the UD57 irradiated sample with $T_c = 25$ K. The full lines are exponential fits according to Eq. (26) which do not take into account the low-field data at low T. For all these samples, we find $H_0 = 25 \pm 5$ T at all temperatures. For the pure UD57 sample, we have also indicated the matching curves taken from Eq. (19) with $H_{c2}(0) = 90(10)$ T in order to better visualize the deviations at larger fields. Here again it is seen that Eq. (19) does not fit the data for $T \gtrsim 93.3$ K, even at low fields, if one keeps the same value of $H_{c2}(0)$ (see discussion in Sec. VIII). The plotted curves correspond to increasing temperatures from top to bottom.

This sharp exponential decay confirms that $H_c'(T)$ can indeed be reliably defined and is not so dependent on the criterion used [we defined it here and in Ref. 16 for $\Delta\sigma_{SF} = 1 \times 10^3(\Omega\,\mathrm{m})^{-1}$].

In order to better visualize how the SCFs are suppressed by magnetic fields in the whole T range, we have then plotted $\Delta\sigma_{SF}$ versus H^2 in a semilogarithmic scale in Fig. 26(b) for the UD85 sample. For the lowest temperatures, we find that Eq. (19) applies with $H_{c2} = 125(5)$ T as long as $H < H^\star$. It is intriguing to see on this plot that the decay of $\Delta\sigma_{SF}$ evolves then smoothly toward an exponential behavior with nearly the same value of H_0 as found at higher temperatures. The same type of evolution is observed for all the samples, pure or irradiated. H_0 remains nearly constant whatever the temperature, doping, or disorder level with $H_0 = 25 \pm 5$ T, as can be seen in Fig. 27.

To conclude, all these experimental observations allow us to establish unambiguously that $H_c'(T)$ sharply delimits a region of the phase diagram beyond which SCFs become vanishling small.

IX. DISCUSSION AND CONCLUSIONS

We have done here a set of measurements where the normal-state MR of $YBa_2Cu_3O_{6+x}$ could be followed down in temperature from the high-T totally non-superconducting state. This allowed us to monitor the progressive advent of fluctuation contributions to the conductivity above T_c. We could not therefore study the close vicinity of T_c, that is, the 3D critical exponents. However, this experiment quite uniquely allowed us to study the variation of SCFs from the 3D to the 2D higher T regime. We could evidence that the GL regime applies

near T_c for optimally doped samples, while for underdoped ones phase fluctuations might play a role in a narrow T range above T_c. Above those T ranges the SCFs are highly damped, which reveals the intrinsic microscopic limitations of the pairing at high temperatures. We have also evidenced that disorder increases the phase-fluctuation regime above T_c. We summarize below the most important conclusions and questions which arise from this work.

Normal-state properties in the pseudogap phase. In Sec. III we definitely evidenced that a 60-T field is not sufficient to suppress totally the 3D SC at T_c in the pure 123 phases, even for underdoped samples with $T_c \simeq 60$ K, so that the normal-state transport properties are only accessible above. The SCFs could only be suppressed fully with 60 T in the presence of strong disorder reducing T_c down to ∼4 K.

In the pure UD57 sample we had demonstrated that the resistivity keeps a metallic behavior at low T in large applied fields.[31] This hole content is slightly lower than that on which maximal quantum oscillations have been observed at low T and high applied fields.[43] From the negative Hall effect detected in these experiments,[44] a reconstruction of the Fermi surface with the appearance of an electron pocket has been proposed. Here we evidenced that the simple relation between the MR and the Hall effect which had been established above ∼130 K in the past[39] has a validity which extends nearly down to T_c, without any singular behavior both for this $YBCO_{6.6}$ composition and for an optimally doped sample. This is in rather good agreement with the fact that, for underdoped $T_c = 57$ K samples, the high-field Hall constant becomes negative only below the zero-field T_c and that the Fermi surface reconstruction only arises deep in the SC state in fields which are, however, insufficient to totally suppress the SCFs.

Ginzburg-Landau regime: Critical fields and gaps. For samples around optimal doping, the quantitative comparative analysis of the measured SCF contribution to the zero-field conductivity and of the off-diagonal Peltier term α_{xy} has been found in total agreement with the GL approach for 2D Gaussian order parameter fluctuations (Sec. VI B). The data perfectly fit the leading order 2D AL contribution up to $T \simeq 1.1T_c$ using the c lattice constant as the mean spacing between the CuO_2 bilayers. It can be fitted as well up to $\sim 1.2T_c$ if higher-order corrections are taken into account. This analysis allows us to deduce values of $\xi(0)$ and of $H_{c2}(0)$ versus doping.

The analysis of the fluctuation magnetoconductivity in this GL regime allows us to determine $H_{c2}(0)$ independently in Sec. VII. The good agreement between these different values establishes the perfect consistency of our data analyses. A very important result obtained here is that the deduced *superconducting gap increases smoothly with increasing hole doping from the underdoped to the overdoped regime*.

Let us recall that energy-resolved spectroscopies have evidenced spectral gaps in the SC state which increase with decreasing doping while here we find a gap which rather follows the same trend as T_c. For overdoped samples the local density of states (LDOS) has coherence peaks[3,72] and exhibits the **k** dependence expected for d wave pairing, which distinguishes the nodal and antinodal regions.[4] Above T_c a small dip in the LDOS remains and has been assigned to the pseudogap, but should be attributed to SCFs, as we have shown that in this range the pseudogap disappears.[16]

However, in the underdoped cases a large gap is found to persist then well above T_c, while at low energies the LDOS becomes nearly independent of local disorder.[73,80] A large debate has been raging recently as various spectroscopy data have suggested that a smaller gap exists, visualized in the nodal regions by Raman spectroscopy[81] or obtained by discriminating different spectral weights in the ARPES or STM spectra.[73,82] Our deduction here, that an important SC property deduced from thermodynamic considerations, that is, the critical field $H_{c2}(0)$, is governed by a gap which follows T_c, reinforces then the idea that *the pseudogap is connected with the large gap detected by STM and ARPES on cuprate sample surfaces in the underdoped regions of their phase diagram*. Conversely, it can be seen that the gap magnitudes deduced from our data scale quite nicely with the smaller gaps obtained by STM.[72,73]

Phase coherence and phase fluctuations. For the $T_c = 57$ K underdoped sample, well into the pseudogap phase, the SCF paraconductivity and Nernst coefficient are found in Sec. VI C both much larger than expected for Gaussian fluctuations in a range of temperatures of the order of 15 K above T_c, which points for the occurrence of phase fluctuations. This range increases markedly if disorder is used to decrease T_c and can become as large as 40 K when T_c has been depressed down to $T_c = 5$ K. These results are therefore consistent with the proposal done by Emery and Kivelson[9] that, in the underdoped regime, controlled disorder reduces the phase coherence. The regime where phase fluctuations might play an important role occurs then between the 3D T_c up to a mean-field temperature which we can assimilate to T_{c0}. In this limited T range we do not have sufficiently accurate measurements nor theoretically established firm criteria to go beyond qualitative observations.

We noticed, however, that the Nernst signal is more enhanced than the excess fluctuation conductivity with respect to expectations for Gaussian fluctuations. More work, both theoretical and experimental, is required to decide the possible importance of vortex contributions to the Nernst effect in this phase-fluctuation regime and/or other possibilities such as the enhancement of SCFs by AF spin fluctuations.[83] However, this enhancement of Nernst effect with respect to excess conductivity decreases for $T > T_{c0}$. So while it has been recently proposed that Nernst measurements were among the best approaches to probe the extension of the SCFs above T_c (Ref. 6), we demonstrated here that those are indeed not as powerful as expected initially for pure YBCO as they are limited by the need of an independent determination of the normal-state Nernst coefficient. The latter is not as small as could be anticipated from the Sondheimer cancellation rule, which applies only for classical metals.[84,85] For the conductivity measurements, our approach using high fields and the former knowledge of the high-T MR permitted to circumvent the corresponding difficulties, so that the SCFs could be followed until they are fully suppressed at high T.

Suppression of SCFs at high T and pairing energies. We have evidenced that in all samples, pure or disordered, and for all dopings, the SCFs sharply decay with increasing T or H, in the ranges where SC Gaussian fluctuations are dominant. In Sec. IV B, we could then deduce for all the samples a curve $H'_c(T)$ ending at $H'_c(T'_c) = 0$, which delineates the (H,T) plane region beyond which SCFs are totally suppressed.

In Sec. VI A, the SCFs are found to be much more rapidly depressed than in thin films of classical s-wave metallic superconductors for which SCFs are detected even for $T \gg T_c$ (Ref. 18). This provides a strong support for our preliminary suggestion[31] that the $H_c'(T)$ curve delineates the regime where microscopic considerations specific to the cuprate physics prohibit SC pairing. We propose in Sec. VIII A that the spatial pair extension at high T is limited by the actual density of carriers available for pairing, *so that a lower bound of* $\xi(T)$ *could be linked with the distance between doped holes*.

The suppression of the fluctuation conductivity is found in Sec. VIII to display a phenomenological exponential decay in $\exp[-(T_c - T_{GL})/T_0]$ and $\exp[-(H/H_0)^2]$, with values of T_0 and H_0 which are not markedly dependent on the doping and disorder. This suggests as well that there is a sharp energy cutoff at $k_B T_c'$ which is shifted by the magnetic energy increase which scales with H_0^2. The energy balance is such that SC pairs cannot be thermally excited any more above T_c' or $H_c'(T)$. Let us notice as well that the extrapolated values of $H_c'(0)$ have been found to be nearly identical to those obtained for $H_{c2}(0)$, which gives confirmation that *both are connected with the pairing energy*. All these consistent deductions give weight to the present analysis.

Influence of disorder and generic PD of cuprates. It has been found by STM that cuprates (or at least Bi2212 surfaces) displayed a short-range disorder, visible, for instance, as a spatial distribution of spectral gaps.[86] These observations have been questioned as being nongeneric, as NMR data indicate that YBCO is not as disordered,[87] hence the metallic behavior observed for $YBCO_{6.6}$ (Ref. 31). This has justified our use of YBCO to study the pure cuprate behavior and the incidence of disorder.[36] We have as well shown that controlled disorder affects drastically the transport properties. Indeed, similar upturns of $\rho(T)$ have been found for controlled disorder in YBCO and in some pure cuprate families, which indicated the occurrence of intrinsic disorder in those families.[46]

The influence of such disorder on SCFs has been thoroughly studied in Sec. IV C and we have shown that the local pair formation emphasized by the T_c' line is only moderately affected, while the bulk T_c, that is, the SC pair coherence, can be severely reduced by disorder. Our results allow us to draw important conclusions on the cuprate phase diagram which we had specifically emphasized in a preliminary report.[16] We could determine that the pseudogap line crosses the T_c' line at optimal doping, which establishes unambiguously that the pseudogap is not the onset of pairing. The results presented here reinforce completely this conclusion as *the fluctuations are similarly limited in field and temperature independently of the pseudogap*, though they are enhanced in magnitude in the underdoped regime.

We want to insist here that specific effects induced by disorder are certainly at the origin of many confusions in the study of High T_c superconductors (HTSC). It is interesting to mention here very recent STM data taken on classical metallic films in presence of large disorder.[88] LDOS measurements reveal strong spatial inhomogeneities of the superconducting gap. The remarkable finding is that the gap magnitude is not much affected when increasing T through T_c while the coherence peaks in the one-particle LDOS disappear. While pairs should be thermally excited and fluctuating above T_c, those appear to be localized by disorder as preformed pairs. The authors call "pseudogap" the reduction of LDOS detected above T_c (Ref. 90). This gap, which is induced by superconducting fluctuations and favored by the vicinity of the superconductor insulator transition in the most disordered samples, has no relation with the situation encountered in clean HTSC, for which the pseudogap is not due to SC pairing and has no connection whatsoever with disorder.[33] This experiment is, however, quite striking as it demonstrates how disorder can produce phenomena which can be easily confused with the pseudogap which characterizes the properties of clean cuprates.

This reinforces our insistence that the cuprate phase diagram has to take into account the presence of disorder, which we have long suggested explains the anomalously low optimum T_c value in some cuprate families. This 3D phase diagram that we anticipated from previous results probing the metal insulator transition[46] and from the recent comparison of T_c and T^* is displayed in Fig. 28. There, in the pure high-T_c systems the occurrence of SCFs and the difficulty to separate the SC gap from the pseudogap in zero-field experiments justifies that the T_c line could often be mistaken as a continuation of the T^* line. It can be also seen there that the respective evolutions with disorder of the SC dome and of the amplitude of the SCF range explains as well the phase diagram often shown in a low-T_c cuprate family such as Bi2201.[89] There both T^* and T_c' might appear well above the shrunken SC dome probably because the actual concentration of carriers is not determined independently but just mapped from the shape of the SC dome.[32] Finally, for intermediate

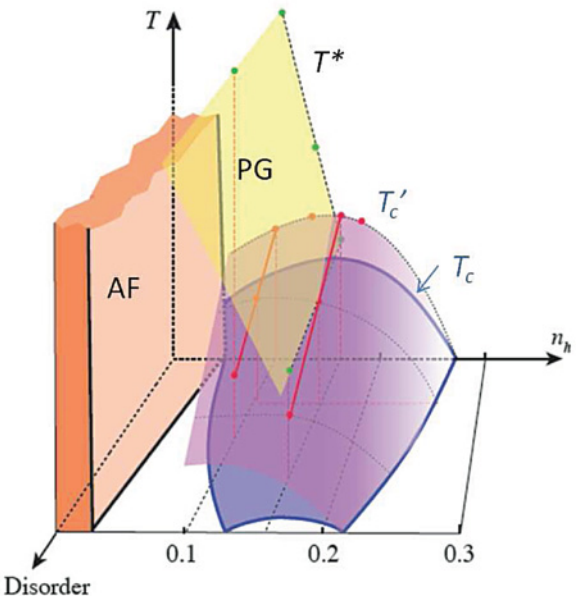

FIG. 28. (Color online) Phase diagram constructed on the data points obtained here, showing the evolution of T_c' and the onset of SCFs, with doping and disorder. The fact that the pseudogap and the SCF surfaces intersect near optimum doping in the clean limit is apparent. These surfaces have been limited to experimental ranges where they have been determined experimentally. In the overdoped regime, data taken on Tl 2201 indicates that disorder suppresses SC without any anomalous extension of the SCFs (Ref. 36).

disorder, the enhanced fluctuation regime with respect to T_c illustrated in the initial Nernst measurements performed in the $La_{2-x}Sr_xCuO_4$ family can be reproduced as well.[6]

Conclusion. In the present work we have performed a thorough quantitative study of the SCFs, which establishes that such data give important determinations of some thermodynamic properties of the SC state of high-T_c cuprates. Those are not accessible otherwise, as flux flow dominates near T_c in the vortex liquid phase and the highest fields available so far are not sufficient to reach the normal state at $T = 0$. This is an illustration that the studies of SCFs permit a "fluctuoscopy"[76] of the SC state. It has allowed us to demonstrate that the pairing energy and SC gap both increase with doping, confirming then that the pseudogap is to be assigned to an independent magnetic order or crossover due to the magnetic correlations.

Further experimental work in even higher fields should help to better characterize the regime where disorder governs the SCFs and to decide about the possible relevance of phase fluctuations. The quasiuniversal behaviors found for the suppression of SCFs in both temperature and magnetic fields beyond the GL regime suggests that pairing is prohibited above an energy scale which is directly linked with microscopic parameters responsible for SC in the cuprates.

Theoretical works within the various scenarios proposed to explain HTSC are highly desirable to connect our data with the microscopic parameters which govern the pairing energy. Such an approach might be helpful to discriminate between theories.

ACKNOWLEDGMENTS

We acknowledge D. Colson and A. Forget for providing the single crystals used in this work. We thank C. Proust and B. Vignolle for their help with the high field pulsed experiments. We also thank L. Benfatto for helpful discussions about phase fluctuations and Kosterlitz-Thouless regime, and K. Benhia for discussions about the Gaussian fluctuations in thin films. This work has been performed within the "Triangle de la Physique" and was supported by ANR Grant No. "OXYFONDA" NT05-4 41913. The experiments at LNCMI-Toulouse were funded by the FP7 I3 EuroMagNET.

*florence.albenque-rullier@cea.fr

[1] H. Alloul, T. Ohno, and P. Mendels, Phys. Rev. Lett. **63**, 1700 (1989).
[2] H. Alloul, P. Mendels, H. Casalta, J. F. Marucco, and J. Arabski, Phys. Rev. Lett. **67**, 3140 (1991).
[3] Ch. Renner, B. Revaz, J-Y. Genoud, K. Kadowaki, and O. Fischer, Phys. Rev. Lett. **80**, 149 (1998).
[4] A. Damascelli, Z. Hussain, and Z. X. Shen, Rev. Mod. Phys. **75**, 473 (2003).
[5] C. Capan, K. Behnia, J. Hinderer, A. G. M. Jansen, W. Lang, C. Marcenat, C. Marin, and J. Flouquet, Phys. Rev. Lett. **88**, 056601 (2002).
[6] Y. Wang, L. Li, and N. P. Ong, Phys. Rev. B **73**, 024510 (2006).
[7] F. Rullier-Albenque, R. Tourbot, H. Alloul, P. Lejay, D. Colson, and A. Forget, Phys. Rev. Lett. **96**, 067002 (2006).
[8] J. Corson, R. Mallozzi, J. Orenstein, J. N. Eckstein, and I. Bozovic, Nature (London) **398**, 221 (1999).
[9] V. J. Emery and S. A. Kivelson, Nature (London) **374**, 434 (1995).
[10] Yayu Wang, Lu Li, M. J. Naughton, G. D. Gu, S. Uchida, and N. P. Ong, Phys. Rev. Lett. **95**, 247002 (2005).
[11] L. Li, Y. Wang, S. Komiya, S. Ono, Y. Ando, G. D. Gu, and N. P. Ong, Phys. Rev. B **81**, 054510 (2010).
[12] V. J. Emery, S. A. Kivelson, and J. M. Tranquada, Proc. Natl. Acad. Sci. USA **96**, 8814 (1999).
[13] T. Hanaguri, C. Lupien, Y. Kohsaka, D.-H. Lee, M. Azuma, M. Takano, H. Takagi, and J. C. Davis, Nature (London) **430**, 1001 (2004); M. J. Lawler, K. Fujita, Jhinhwan Lee, A. R. Schmidt, Y. Kohsaka, Chung Koo Kim, H. Eisaki, S. Uchida, J. C. Davis, J. P. Sethna, and Eun-Ah Kim, *ibid*. **466**, 347 (2010).
[14] C. M. Varma, Phys. Rev. B **55**, 14554 (1997); Phys. Rev. Lett. **83**, 3538 (1999).
[15] P. Bourges and Y. Sidis, Comptes Rendus Physique **12**, 461 (2011).
[16] H. Alloul, F. Rullier-Albenque, B. Vignolle, D. Colson, and A. Forget, Europhys. Lett. **91**, 37005 (2010).
[17] W. J. Skocpol and M. Tinkham, Rep. Prog. Phys. **38**, 1049 (1975).
[18] A. Pourret, H. Aubin, J. Lesueur, C. A. Marrache-kikuchi, L. Bergé, L. Dumoulin, and K. Behnia, Nat. Phys. **2**, 683 (2006).
[19] A. Pourret, P. Spathis, H. Aubin, and K. Behnia, New J. Phys. **11**, 055071 (2009).
[20] For a review see, A. Larkin and A. A. Varlamov, *Theory of Fluctuations in Superconductors* (Oxford University Press, Oxford, 2005).
[21] R. Hopfengartner, B. Hensel, and G. Saemann-Ischenko, Phys. Rev. B **44**, 741 (1991).
[22] P. Mandal *et al*., Physica C **169**, 43 (1990).
[23] H. M. Duan, W. Kiehl, C. Dong, A. W. Cordes, M. J. Saeed, D. L. Viar, and A. M. Hermann, Phys. Rev. B **43**, 12925 (1991).
[24] M. R. Cimberle, C. Ferdeghini, E. Giannini, D. Marre, M. Putti, A. Siri, F. Federici, and A. Varlamov, Phys. Rev. B **55**, R14745 (1997).
[25] W. Lang, G. Heine, W. Kula, and R. Sobolewski, Phys. Rev. B **51**, 9180 (1995).
[26] K. Semba, T. Ishii, and A. Matsuda, Phys. Rev. Lett. **67**, 769 (1991).
[27] W. Holm, O. Rapp, C. N. L. Johnson, and U. Helmersson, Phys. Rev. B **52**, 3748 (1995).
[28] F. Bouquet, L. Fruchter, I. Sfar, Z. Z. Li, and H. Raffy, Phys. Rev. B **74**, 064513 (2006).
[29] C. Sekirnjak, W. Lang, S. Proyer, and P. Schwab, Physica C **243**, 60 (1995).
[30] Y. Ando and K. Segawa, Phys. Rev. Lett. **88**, 167005 (2002).
[31] F. Rullier-Albenque, H. Alloul, Cyril Proust, P. Lejay, A. Forget, and D. Colson, Phys. Rev. Lett. **99**, 027003 (2007).
[32] J. L. Tallon, C. Bernhard, H. Shaked, R. L. Hitterman, and J. D. Jorgensen, Phys. Rev. B **51**, 12911 (1995).
[33] H. Alloul, J. Bobroff, M. Gabay, and P. Hirschfeld, Rev. Mod. Phys. **81**, 45 (2009).

[34]A. Legris, F. Rullier-Albenque, E. Radeva, and P. Lejay, J. Phys. I (France) **3**, 1605 (1993).
[35]F. Rullier-Albenque, P. A. Vieillefond, H. Alloul, A. W. Tyler, P. Lejay, and J. F. Marucco, Europhys. Lett. **50**, 81 (2000).
[36]F. Rullier-Albenque, H. Alloul, and R. Tourbot, Phys. Rev. Lett. **87**, 157001 (2001).
[37]F. Rullier-Albenque, H. Alloul, and R. Tourbot, Phys. Rev. Lett. **91**, 047001 (2003).
[38]A. Lacerda, J. P. Rodriguez, M. F. Hundley, Z. Fisk, P. C. Canfield, J. D. Thompson, and S. W. Cheong, Phys. Rev. B **49**, 9097 (1994).
[39]J. M. Harris, Y. F. Yan, P. Matl, N. P. Ong, P. W. Anderson, T. Kimura, and K. Kitazawa, Phys. Rev. Lett. **75**, 1391 (1995).
[40]Z. Konstantinovic, O. Laborde, P. Monceau, Z. Z. Li, and H. Raffy, Physica B **259–261**, 569 (1999).
[41]A. W. Tyler, Ph.D. thesis, University of Cambridge, 1997.
[42]For the underdoped sample, the longitudinal MR component has been shown to be significant at high temperature.[39] We did not measure it but assume here that it remains quadratic in field up to 60 T. Any saturation of this MR would only marginally change the results.
[43]N. Doiron-Leyraud, C. Proust, D. LeBoeuf, J. Levallois, J.-B. Bonnemaison, R. Liang, D. A. Bonn, W. N. Hardy, and L. Taillefer, Nature **447**, 565 (2007).
[44]D. LeBoeuf, N. Doiron-Leyraud, J. Levallois, R. Daou, J.-B. Bonnemaison, N. E. Hussey, L. Balicas, B. J. Ramshaw, Ruixing Liang, D. A. Bonn, W. N. Hardy, S. Adachi, C. Proust, and L. Taillefer, Nature **450**, 533 (2007).
[45]In the case of the OPT93.6 and UD57 samples, we have added data taken in a range where the magnetic field is not actually large enough to totally suppress the SC. At each T, we have used the corresponding value of $a_{\rm trans}$ by extrapolating the curve of Fig. 4 and calculated the curve of the normal-state resistivity versus magnetic field with different values of ρ_n for the highest applied magnetic field. This allows us to deduce values of $\Delta\sigma_{SF}(T,0)$ within the indicated error bars.
[46]F. Rullier-Albenque, H. Alloul, F. Balakirev, and C. Proust, Europhys. Lett. **81**, 37008 (2008).
[47]N. Bergeal, J. Lesueur, M. Aprili, G. Faini, J. P. Contour, and B. Leridon, Nat. Phys. **4**, 608 (2008).
[48]M. S. Grbić, M. Požek, D. Paar, V. Hinkov, M. Raichle, D. Haug, B. Keimer, N. Barišić, and A. Dulčić, Phys. Rev. B **83**, 144508 (2011).
[49]M. S. Grbić, N. Barišić, A. Dulčić, I. Kupčić, Y. Li, X. Zhao, G. Yu, M. Dressel, M. Greven, and M. Požek, Phys. Rev. B **80**, 094511 (2010).
[50]Y. Wang, S. Ono, Y. Onose, G. Gu, Y. Ando, Y. Tokura, S. Uchida, and N. P. Ong, Science **299**, 86 (2003).
[51]L. Li, Y. Wang, J. G. Checkelsky, M. J. Naughton, S. Komiya, S. Ono, Y. Ando and N. P. Ong, Physica C **460–462**, 48 (2007).
[52]A. Pourret, H. Aubin, J. Lesueur, C. A. Marrache-Kikuchi, L. Bergé, L. Dumoulin, and K. Behnia, Phys. Rev. B **76**, 214504 (2007).
[53]S. K. Yip, Phys. Rev. B **41**, 2612 (1990).
[54]W. E. Lawrence and S. Doniach, in *Proceedings 12th International Conference on Low Temperature Physics, Kyoto 1970*, edited by E. Kanda (Keigaku, Tokyo, 1971), p. 361.
[55]P. P. Freitas, C. C. Tsuei, and T. S. Plaskett, Phys. Rev. B **36**, 833 (1987).
[56]R. Hopfengärtner, B. Hensel, and G. Saemann-Ischenko, Phys. Rev. B **44**, 741 (1991).
[57]A. Gauzzi and D. Pavuna, Phys. Rev. B **51**, 15420 (1995).
[58]I. Ussishkin, S. L. Sondhi, and D. A. Huse, Phys. Rev. Lett. **89**, 287001 (2002).
[59]B. Leridon, J. Vanacken, T. Wambecq, and V. V. Moshchalkov, Phys. Rev. B **76**, 012503 (2007).
[60]As explained in Ref. 7, the off-diagonal Peltier term α_{xy} is determined from the Nernst coefficient ν, the Hall angle θ_H, the conductivity σ and the thermopower coefficient S as $\alpha_{xy} = \sigma[\nu B + S\tan\theta_H]$.
[61]R. Daou, J. Chang, David LeBoeuf, Olivier Cyr-Choinière, Francis Laliberté, Nicolas Doiron-Leyraud, B. J. Ramshaw, Ruixing Liang, D. A. Bonn, W. N. Hardy, and L. Taillefer, Nature (London) **463**, 519 (2010).
[62]I. Kokanovic, J. R. Cooper, and M. Matusiak, Phys. Rev. Lett. **102**, 187002 (2009).
[63]P. A. Lee, N. Nagaosa, and X. G. Wen, Rev. Mod. Phys. **78**, 17 (2006).
[64]B. I. Halperin and D. R. Nelson, J. Low. Temp. Phys. **36**, 599 (1979).
[65]L. Benfatto, C. Castellani, and T. Giamarchi, Phys. Rev. B **80**, 214506 (2009).
[66]J. L. Tallon, J. G. Storey, and J. W. Loram, Phys. Rev. B **83**, 092505 (2011).
[67]S. Hikami and A. I. Larkin, Mod. Phys. Lett. B **2**, 693 (1988).
[68]Y. Matsuda, T. Hirai, S. Komiyama, T. Terashima, Y. Bando, K. Iijima, K. Yamamoto, and K. Hirata, Phys. Rev. B **40**, 5176 (1989).
[69]A. Kapitulnik, A. Palevski, and G. Deutscher, J. Phys. C **18**, 1305 (1985).
[70]X. J. Zhou, T. Yoshida, A. Lanzara, P. V. Bogdanov, S. A. Kellar, K. M. Shen, W. L. Yang, F. Ronning, T. Sasagawa, T. Kakeshita, T. Noda, H. Eisaki, S. Uchida, C. T. Lin, F. Zhou, J. W. Xiong, W. X. Ti, Z. X. Zhao, A. Fujimori, Z. Hussain, and Z.-X. Shen, Nature (London) **423**, 398 (2003).
[71]D. Fournier, G. Levy, Y. Pennec, J. L. McChesney, A. Bostwick, E. Rotenberg, R. Liang, W. N. Hardy, D. A. Bonn, I. S. Elfimov, and A. Damascelli, Nat. Phys. **6**, 905 (2010).
[72]A. Yazdani, J. Phys. Condens. Matter **21**, 164214 (2009).
[73]M. C. Boyer, W. D. Wise, K. Chatterjee, M. Yi, T. Kondo, T. Takeuchi, H. Ikuta, and E. W. Hudson, Nat. Phys. **3**, 802 (2007).
[74]S. Hüfner, M. A. Hossain, A. Damascelli, and G. A. Sawatzky, Rep. Prog. Phys. **71**, 062501 (2008).
[75]L. Reggiani, R. Vaglio, and A. A. Varlamov, Phys. Rev. B **44**, 9541 (1991).
[76]A. Glatz, A. A. Varlamov, and V. M. Vinokur, e-print arXiv:1012.1104 (to be published).
[77]C. Carballeira, S. R. Curras, J. Viña, J. A. Veira, M. V. Ramallo, and F. Vidal, Phys. Rev. B **63**, 144515 (2001).
[78]F. Vidal, C. Carballeira, S. R. Curras, J. Mosqueira, M. V. Ramallo, J. A. Veira, and J. Vina, Europhys. Lett. **59**, 754 (2002).
[79]Alex Levchenko, M. R. Norman, and A. A. Varlamov, Phys. Rev. B **83**, 020506(R) (2011).
[80]K. McElroy, D.-H. Lee, J. E. Hoffman, K. M. Lang, J. Lee, E. W. Hudson, H. Eisaki, S. Uchida, and J. C. Davis, Phys. Rev. Lett. **94**, 197005 (2005).
[81]M. Le Tacon, A. Sacuto, A. Georges, G. Kottliar, Y. Gallais, D. Colson, and A. Forget, Nat. Phys. **2**, 537 (2006).
[82]T. Kondo, R. Khasanov, T. Takeuchi, J. Schmalian, and A. Kaminski, Nature (London) **457**, 296 (2009).
[83]F. Rullier-Albenque, R. Tourbot, H. Alloul, P. Lejay, D. Colson, and A. Forget, Phys. Rev. Lett. **96**, 067002 (2006).

[84]K. Behnia, J. Phys. Condens. Matter **21**, 113101 (2009).
[85]A. Hackl and M. Vojta, Phys. Rev. B **80**, 220514(R) (2009).
[86]S. H. Pan, J. P. O'Neal, R. L. Badzey, C. Chamon, H. Ding, J. R. Engelbrecht, Z. Wang, H. Eisaki, S. Uchida, A. K. Guptak, K.-W. Ngk, E. W. Hudson, K. M. Lang, and J. C. Davis, Nature (London) **413**, 282 (2001).
[87]J. Bobroff, H. Alloul, S. Ouazi, P. Mendels, A. Mahajan, N. Blanchard, G. Collin, V. Guillen, and J.-F. Marucco, Phys. Rev. Lett. **89**, 157002 (2002).
[88]B. Sacépé, C. Chapelier, T. I. Baturina, V. M. Vinokur, M. R. Baklanov, and M. Sanquer, Phys. Rev. Lett. **101**, 157006 (2008); B. Sacépé, T. Dubouchet, C. Chapelier, M. Sanquer, M. Ovadia, D. Shahar, M. Feigelman, and L. Ioffe, Nat. Phys. **7**, 239 (2011).
[89]Ø. Fischer, M. Kugler, I. Maggio-Aprile, C. Berthod, and C. Renner, Rev. Mod. Phys. **79**, 353 (2007).
[90]B. Sacépé, C. Chapelier, T. I. Baturina, V. M. Vinokur, M. R. Baklanov, and Marc Sanquer, Nat. Commun. **1**, 140 (2010).